



Determination of Residual Stresses in a Carbon-Fibre Reinforced Polymer using the Incremental Hole-Drilling Technique

Author: Smart K Okai

(Student number: 384029)

School of Mechanical, Industrial and Aeronautical Engineering

University of the Witwatersrand,
Johannesburg, South Africa

Supervisor: Professor J.P Nobre

A Research Report submitted to the Faculty of Engineering and the Built Environment, University of the Witwatersrand, in fulfillment of the requirements for the degree of **Master of Science in Engineering(Mechanical Engineering)**

SUBMITTED ON 30TH JANUARY, 2017

DECLARATION

I hereby declare that I am aware that plagiarism (the use of some else's work without their permission and/or without acknowledging the original source) is wrong. I confirm that the work submitted for assessment for the above degree is my own unaided work except where I have explicitly indicated otherwise. It has not been submitted before for any degree or examination at any other University.

Signed thisday of2017

Smart Koranteng Okai

Certified by My Supervisor:
Professor J.P. Nobre

Date_____

DEDICATION

This research project is dedicated to my uncle Mr Seth Kwasi Yeboah for his selfless pieces of advice and encouragement given to me towards the completion of this work. Again it is also dedicated to all best wishers and friends.

ACKNOWLEDGEMENT

Ebenezer, this is how far the lord has brought me. May his name be praised and glorified. I would like to express my profound gratitude to the almighty God for the strength and power given to me to undertake this research work. I am thankful to all those who in one way or the other contributed in the successful completion of this work.

My heartfelt gratitude goes to my supervisor Professor João-Paulo Nobre for his ever willingness to assist; give directions, offer suggestions and pieces of advice, and sharing of knowledge to make this project a success.

ABSTRACT

An extensive variety of experimental techniques exist to determining residual stresses, but few of these techniques is suitable, however, for finding the residual stresses that exist in orthotropic or anisotropic layered materials, such as carbon-fibre reinforced polymers (CFRP). Among these techniques, particularly among the relaxation techniques, the incremental hole-drilling technique (IHD) has shown to be a suitable technique to be developed for this purpose. This technique was standardized for the case of linear elastic isotropic materials, such as the metallic alloys in general. However, its reliable application to anisotropic and layered materials, such as CFRP materials, needs to be better studied. In particular, accurate calculation methods to determine the residual stresses in these materials based on the measured in-depth strain relaxation curves need to be developed.

In this work, existing calculation methods and already proposed theoretical approaches to determine residual stresses in composite laminates by the incremental hole-drilling technique are reviewed. The selected residual stress calculation method is implemented using MATLAB. For these calculations, specific calibration coefficients have to be numerically determined by the finite element method, using the ANSYS software. The developed MATLAB scripts are then validated using an experimental procedure previously developed. This experimental procedure was performed using CFRP specimens, with the stacking sequence $[0^\circ, 90^\circ]_{5s}$ and, therefore, this composite laminate was selected as case study in this work.

Some discrepancies between the calculated stresses using the MATLAB scripts and those imposed during the experimental calibration procedure are observed. The errors found could be explained considering the limitations inherent to the incremental hole-drilling technique and the theoretical approach followed. However, the obtained results showed that the incremental hole-drilling can be considered a promising technique for residual stress measurement in composite laminates.

Keywords: residual stress, carbon fibre reinforced polymer, incremental hold drilling technique.

TABLE OF CONTENTS

TITLE PAGE	
DECLARATION.....	i
DEDICATION	ii
ACKNOWLEDGEMENT.....	iii
ABSTRACT.....	iv
TABLE OF CONTENT.....	v
LIST OF FIGURES.....	viii
LIST OF TABLES.....	x
NOMENCLATURE.....	xi
1. INTRODUCTION.....	1
1.1 Purpose of the research.....	2
1.2 Research motivation.....	2
1.3 Problem statement.....	3
2. LITERATURE REVIEW.....	3
2.1 Introduction.....	3
2.2 Fibre reinforced polymers.....	4
2.3 Carbon fibre reinforced polymers (CFRP).....	5
2.4 Classification and types of carbon fibres	6
2.5 Isotropic materials and anisotropic materials.....	7
2.6 Available techniques for residual stress determination in CFRP.....	8
2.6.1 First ply failure.....	9
2.6.2 Hole-drilling technique.....	9
2.6.3 Ring Core method.....	12
2.6.4 The slitting method or Crack compliance method.....	12
2.6.5 Layer removal Method.....	13
2.6.6 Deep hole method.....	13
2.6.7 Sachs Method.....	14

2.7 The incremental hole-drilling technique and its application to composite laminates.....	15
2.7.1 Introduction.....	15
2.7.2 Strain gauge rosettes.....	17
2.7.3 Residual stress evaluation procedures for orthotropic/anisotropic layered material..	18
3. RESEARCH AIMS AND OBJECTIVES.....	23
4. RESEARCH AIMS AND OBJECTIVES.....	23
5. RESEARCH METHODS.....	24
5.1 Numerical procedure.....	24
5.1.1 Introduction.....	24
5.1.2 Determination of Calibration coefficients.....	25
5.2 Materials and experimental procedure.....	26
5.2.1 Material and specimens.....	26
5.2.2 Brief description of the experimental procedure used for validation purposes.....	27
5.2.3 Incremental hole-drilling parameters.....	30
6. MATLAB SCRIPT DEVELOPMENT.....	31
7. RESULTS AND DISCUSSION.....	34
7.1 Calibration coefficient matrices.....	34
7.2 Experimental in-depth strain relaxation distribution.....	42
7.3 Calculated stress distribution and validation of the MATLAB scripts developed.....	44
7.3.1 Effect of the drill bit geometry.....	46
7.3.2 Effect of the numerical uncertainties.....	47
7.3.3 Thermo-mechanical effects of the cutting procedure.....	48
7.3.4 Limitation of the theoretical approach used for residual stress calculation.....	48
8. CONCLUSION.....	49

9. REFERENCES.....51

10. APPENDIX.....55

LIST OF FIGURES

Figure 2.1: Carbon fibre reinforced composite.....	5
Figure 2.2: composite materials constituents. [13].....	5
Figure 2.3: Relative locations of the hole and the strain (figure from [21]).....	11
Figure 2.4: schematic diagram of the slitting method.....	13
Figure 2.5: a schematic diagram of the Sachs Method.....	15
Figure 2.6: Incremental hole-drilling technique instruments use for the determination of residual stresses in carbon fibre reinforced polymer: SINT MTS3000 (left) and Vishay MS200 milling guide (right).....	17
Figure 2.7: Three strain gauges rosettes existing in the ASTM E837-13 [33].....	18
Figure 2.8: Strain gauge rosette arrangements placed around where the hole was to be drilled for determining residual stress[41].....	20
Figure 5.1: Finite element models after the first increment [3].....	25
Figure 5.2: Fifth drilling stage.....	26
Figure 5.3: Superposition principle to eliminate the initial residual stresses.....	28
Figure 5.4: Sequence of applied load cycles during the calibration procedure	29
Figure 5.5: The coordinate system, the hole geometry and the position three-clockwise (CW) strain gauge rosette for the incremental hole-drilling method [25].....	31
Figure 7.1: 3D finite element mesh used in the FEM simulation of the $[0/90]_{5s}$ composite laminate.....	35
Figure 7.2: 3D finite element mesh used in the hole-drilling FEM simulation of the $[0/90]_{5s}$ composite laminate (closer view) – two depth increments per ply were used.....	35
Figure 7.3: Relative size of the strain gauge area in the 3D finite element mesh used in the hole- drilling FEM simulation of the $[0/90]_{5s}$ composite laminate (1mm hole-depth).....	36
Figure 7.4: von Mises stress field (left) and strain field during the determination of the coefficient constants matrix A_{in} (1mm hole-depth).....	37
Figure 7.5: Strain relaxation against depth increment generated using MATLAB code.....	43
Figure 7.6: Minimum principal stresses and maximum principal stresses calculated by the MATLAB scripts developed	44

Figure 7.7: Observed error [%] between the maximum principal stress calculated by the MATLAB scripts developed and the expected stress value.....46

Figure 7.8: Micrograph of a drilled hole showing the remaining portion which was not removed [45]41

Figure 7.9: Angular variation of relieved strain in materials of varying degree of axial orthotropy. ASTM strain gauge geometry. [33].....44

LIST OF TABLES

Table 5.1 Properties of the material used in the test [43].....	27
Table 5.2 incremental hole-drilling parameters previously used during the tests [32, 43].....	30
Table 7.1 – Calibration coefficient matrix A_{in}	39
Table 7.2 – Calibration coefficient matrix B_{in}	40
Table 7.3 – Calibration coefficient matrix C_{in}	41
Table 7.4 Strain-depth relaxation values obtained during the experimental calibration [40].....	42

NOMENCLATURE

Symbols/abbreviations	Descriptions	Unit
ASTM	American Society of Testing and Materials	
CFRP	Carbon fibre reinforced polymer	-
FEM	Finite Element Method	
PMC	Polymer Matrix Composite	-
IHDT	Incremental hole drilling technique	-
IHD	Incremental hole drilling	-
HDM	Hole drilling method	-
UHM	Ultra-high-modulus	
PAN	polyacrylonitrile	
HM	High-modulus, type HM	
IM	Intermediate-modulus, type	
HT	High-Tensile,	
SHT	Super high-tensile	
IHT	Intermediate-heat-treatment	
MPa	Mega Pascal	MPa
GPa	Giga Pascal	GPa
σ_{1hi}	Longitudinal stress	MPa
σ_{2hi}	Transverse stress	MPa
A_{in}	Calibration Constant	
B_{in}	Calibration Constant	
C_{in}	Calibration Constant	
FEA	Finite element analysis	
E_L	Elastic limit in the longitudinal direction	
E_T	Elastic limit in the transverse direction	

1. INTRODUCTION

Carbon Fibre Reinforced Polymer (CFRP) is a Polymer Matrix Composite (PMC) material reinforced by carbon fibers. The carbon fibres possess the highest specific mechanical properties such as modulus of elasticity and strength. Because CFRP are characterized by the following mechanical properties: light in weight, high strength to weight ratio, very high modulus of elasticity to weight ratio, high fatigue strength, good corrosion resistance, very low coefficient of thermal expansion and low impact resistance, they are perfect choice for a large number of structural applications, ranging from aircraft, helicopters and spacecraft through to boats, ships and offshore platforms and to automobiles, sports goods, chemical processing equipment and civil infrastructure such as bridges and buildings.

Residual stresses are normally stresses that build up or remain in equilibrium in a solid material without the application of external loads. They can be found in most composite laminates. During manufacturing or operation of the composite structure, residual stresses can be developed in either process, due to different coefficients of thermal expansion of matrix and fibres or the curing process. Since residual stresses can be a large magnitude they may affect the strength of composite structures and their external load bearing capacity [1].

Notwithstanding how they are formed, residual stresses in carbon fibre reinforced polymer (CFRP) adversely impact on the mechanical performance of composites and it is necessary to develop techniques to characterize them before these materials are placed in service. Residual stresses can cause failure of a part below the design load or, under fatigue loading, when neglected during design, prior to the useful design life of the part [2, 3].

There are a lot of techniques which are used to determine residual stresses in composite materials. Generally, the experimental techniques used for the estimation of residual stresses are divided into three categories: destructive, semi-destructive and non-destructive. The method that will be used for this research paper for the determination of residual stresses in CFRP is the incremental hole-drilling technique (IHDT), which is a semi-destructive (relaxation) technique. The IHDT is categorized as semi-destructive because a small hole is drilled into the component. This technique has been shown by researchers to appear to be a promising technique for measuring in-depth non-uniform residual

stresses in CFRP [4, 5]. In composite laminates which are orthotropic in nature, residual stresses are not-homogeneous in the through-thickness, in which case the Standard Test Method for Determining Residual Stresses by the hole-drilling strain-gauge method according to (ASTM E-837) standards cannot be applied because it is only valid for homogenous and isotropic materials. In the case of orthotropic materials which are non-uniform, such as high-performance (FRP), residual stress can be developed and the evaluation procedure of incremental hole drilling technique should be developed.

1.1 Purpose of the research

The purposes of this research are:

- i. To establish a residual stress calculation procedure for carbon fibre-reinforced polymer using incremental hole-drilling technique and which seems to be a promising technique among all the destructive (relaxation) methods.
- ii. To implement calculation procedures using MATLAB software program to determine residual stresses in carbon fibre reinforced polymer (CFRP).

1.2 Research motivation

- There is no commercial evaluation procedure available for the determination of residual stresses in anisotropic/orthotropic and layered materials, such as CFRP, using the incremental hole-drilling technique.
- This research will extend the ability of Wits University to determine residual stresses using the incremental hole drilling (IHD) technique (SINT MTS3000); the results of this project will aid the School's research in this field.
- Since the formation of residual stresses in CFRP cannot be avoided, there must be a proper experimental evaluation procedure to determine their distribution in the material.
- In order to obtain information of the characteristic generation of residual stresses for explicit manufacturing or process conditions, the dependability of residual stress analysis technique is vital.
- It is necessary to measure residual stresses using experimental methods so as to verify and validate theoretical results as well as to provide a reliable means of residual stress determination and evaluation.

1.3 Problem statement

The hole-drilling method using strain gauges was originally established for isotropic and homogeneous materials in order to determine the uniform residual stresses in the through thickness of the material and further the non uniform residual stress distribution (2008 revision of the American standard ASTM E-837 [33]). However, in the case of orthotropic/anisotropic and layered materials, such as carbon-fibre reinforced polymer (CFRP), there is no standard evaluation procedure for residual stress determination by using the incremental hole-drilling technique.

In this case the technique will be used to:

- Determine the distribution of the residual stresses in the plies of CFRP composite laminates.
- Establish a calibration procedure for residual stress determination.
- Determine specific calibration coefficients by using the finite element method.
- Implement MATLAB scripts for computation of residual stresses.
- Validate the results obtained with experimentally obtained strain-depth relaxation results.

2. LITERATURE REVIEW

2.1 Introduction

Carbon fibre-reinforced polymer (CFRP) is a composite material made of a polymer matrix reinforced with fibres. These materials are increasingly being considered as an enhancement to and/or substitute for infrastructure components stretching from industrial to household applications.

Residual stresses formation in high performance CFRPs are one of the problems that needs to be addressed. They can develop either during manufacturing or operation of the composite structure. Since they can have a large magnitude they may affect the strength of composite structures and their external load bearing capacity. After processing and consequent cooling of the composite laminates from the relatively high processing temperature to the service temperature, residual stresses arise due to the considerably higher contraction of the matrix compared with the fibre [6]. If residual stresses are therefore ignored during design, their influence on the mechanical properties of a part can have a significant impact on the safety, dependability and reliability of structural engineering components.

They can cause failure of a component below the design load or, under the fatigue loading, prior to the useful design life of the component.

Another process by which residual stresses are introduced into CFRP composite laminate is the forming process, which are due to unmatched coefficients of thermal expansion of the plies having different orientations and non-uniform cooling of the component due to severe temperature gradients during manufacturing. The need to employ an appropriate technique to estimate and determine residual stresses in a composite laminate in a material like CFRP is therefore required.

Again, the expansion due to moisture absorption can also bring non-uniform residual stresses in a given ply of a laminate. When several individual laminate are bonded together with their fiber directions at different angles, the inter-laminar residual stress occurs. In the common situation of cool-down, the inherent anisotropic contraction of each ply generates stresses at the junction planes between them. Some of the damage that appears such as: micro-cracking, breaking of fibers and inter-ply delamination, are initiated by residual stresses and external loading [7, 8 - 9].

2.2 Fibre reinforced polymer

Fibre-reinforced polymer (FRP), also known as Fibre-reinforced plastic, is a composite material made of a polymer matrix reinforced with fibres. The fibres are normally glass, carbon, or aramid, although other fibres such as paper or wood or asbestos have been sometimes used. The polymer is usually an epoxy, vinylester or polyester thermosetting plastic, and phenol formaldehyde resins are still in use.

Composite Materials are materials made from two or more constituent materials with significantly different physical or chemical properties which remain separate and distinct within the finished structure, and that, when combined, produce a material with characteristics different from the individual components. The individual components remain separate and distinct within the finished structure. The new material may be preferred for many reasons: common examples include materials which are stronger, lighter, or less expensive when compared to traditional materials. The purpose is usually to make a component which is strong and stiff, often with a low density. Commercial materials commonly have glass or carbon fibres in matrices based on thermosetting polymers, such as epoxy or polyester resins. Sometimes, thermoplastic polymers may be preferred, since they are

moldable after initial production. There are further classes of composite in which the matrix is a metal or a ceramic. For the most part, these are still in a developmental stage, with problems of high manufacturing costs yet to be overcome [10]. Furthermore, in these composites the reasons for adding the fibres (or, in some cases, particles) are often rather complex; for example, improvements may be sought in creep, wear, fracture toughness, thermal stability, etc [11-12].

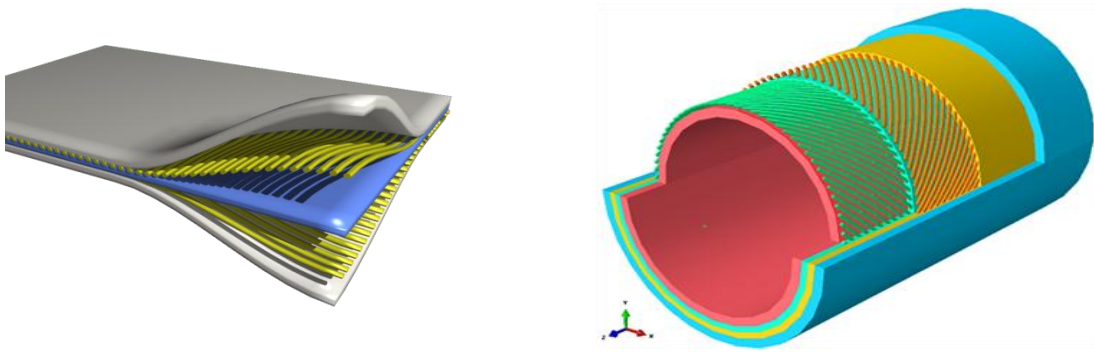


Figure 2.1 Carbon fibre reinforced composite.

The hierarchy that shows constituents of some composite materials is depicted in figure 2.2 below.

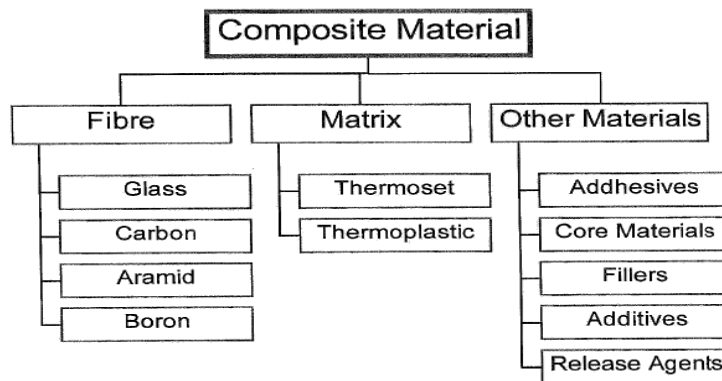


Figure 2.2 composite materials constituents. [13]

2.3 Carbon fibre reinforced polymers (CFRP)

Carbon-fibre-reinforced polymer or carbon-fibre-reinforced plastic (CFRP or CRP or often simply carbon fibre), is a very strong and light fibre-reinforced polymer which contains carbon fibres. Carbon fibres are created when polyacrylonitrile fibres (PAN), Pitch resins, or Rayon are carbonized

(through oxidation and thermal pyrolysis) at high temperatures. Through further processes of graphitizing or stretching the fibres strength or elasticity can be enhanced respectively. Carbon fibres are manufactured in diameters analogous to glass fibres with diameters ranging from 9 to 17 μm . These fibres wound into larger threads for transportation and further production processes. Further production processes include weaving or braiding into carbon fabrics, cloths and mats equivalent to those described for glass that can then be used in actual reinforcement processes. Carbon fibres are a new breed of high-strength materials. Carbon fibre has been described as a fibre containing at least 90% carbon obtained by the controlled pyrolysis of appropriate fibres. The existence of carbon fibre came into being in 1879 when Edison took out a patent for the manufacture of carbon filaments suitable for use in electric lamps [14].

The main matrix materials for producing Carbon Fiber Reinforced Polymers (CFRP) are thermosetting such as epoxy, polyester and thermoplastics such as nylon (polyamide). CFRP materials usually have laminate structure, providing reinforcing in two perpendicular directions and the materials usually have laminate structure, providing reinforcing in two perpendicular directions. Because of their numerous usages in the engineering field, the residual stress which influence the properties of the composite structures significantly have to be taken into account in both design and numerical modeling. Consequently the study and the knowledge of mechanical behavior and strength of composite structures fundamentally imply accurate determination of the residual stress condition.

2.4 Classification and types of carbon fibres

Carbon fibres can be classified into the following categories based on their modulus, strength, and final heat treatment temperatures:

2.4.1 Carbon fibre can be grouped into the following based on their carbon fibre properties:

- Ultra-high-modulus, type UHM (modulus $>450\text{Gpa}$)
- High-modulus, type HM (modulus between 350-450Gpa)
- Intermediate-modulus, type IM (modulus between 200-350Gpa)
- Low modulus and high-tensile, type HT (modulus $< 100\text{Gpa}$, tensile strength $> 3.0\text{Gpa}$)
- Super high-tensile, type SHT (tensile strength $> 4.5\text{Gpa}$)

2.4.2 Based on precursor fiber materials, carbon fibers are classified into;

- PAN-based carbon fibres

- Pitch-based carbon fibres
- Mesophase pitch-based carbon fibres
- Isotropic pitch-based carbon fibres
- Rayon-based carbon fibers
- Gas-phase-grown carbon fibres

2.4.3 Based on final heat treatment temperature, carbon fibres are classified into:

- Type-I, high-heat-treatment carbon fibers (HTT), where final heat treatment temperature should be above 2000°C and can be associated with high-modulus type fibre.
- Type-II, intermediate-heat-treatment carbon fibres (IHT), where final heat treatment temperature should be around or above 1500 °C and can be associated with high-strength type fibre.
- Type-III, low-heat-treatment carbon fibres, where final heat treatment temperatures not greater than 1000 °C. These are low modulus and low strength materials [15].

2.5 Isotropic materials and anisotropic materials

Materials are said to be isotropic if the properties are not dependent on the directions, which means having identical values of a property in all directions. In isotropic materials, physical and mechanical properties are equal in all orientations or directions. Properties like Young's modulus, thermal expansion coefficient, Poisson's ratio, shear modulus of elasticity mass density, yield strength do not change in the directions of isotropic materials. Isotropic materials can be homogeneous or non-homogeneous microscopic structure.

Anisotropic materials have different physical properties in different directions relative to the crystal orientation of the materials. For example, the Young's modulus of single crystalline silicon depends on the measurement direction relative to the crystal orientation. Anisotropic material's properties such as Young's Modulus, coefficient of thermal expansion and magnetic properties change with direction along the object. Common examples of anisotropic materials are wood and composites. Therefore, when designing mechanical structures using anisotropic mechanical materials, the designer should be aware of the orientation relation between the mechanical structure and the material crystals, and specify the relation in the simulation settings.

Directionally dependent physical properties of anisotropic materials are significant due to the affects it has on how the material behaves. For example, in the case of fracture mechanics, the way the microstructure of the material is oriented will affect the strength and stiffness of the material in various directions therefore affecting direction of crack growth.

Anisotropic materials, naturally and artificial, are used in numerous areas of study. Some examples are Magnetic anisotropy in which the magnetic field is oriented in a preferred direction, anisotropic heat conduction that is dependent on the geometry and or anisotropic material. Anisotropic materials are also a result of manufacturing of materials such as a rolling or deep-drawing process. Composites and other materials are used and altered for specific applications.

2.6 Available techniques for residual stress determination in CFRP

There are a range of existing techniques to estimate and determine residual stresses in composite laminates. Most of these techniques are used for isotropic and homogeneous materials for the uniform determination of residual stresses in through-thickness of the materials. The incremental hole-drilling technique appears to be a promising technique, in the case of orthotropic materials, to determine residual stresses in every part of the component [16]. The principle used to determine the stress is the same as that of the promising hole drilling method, but in this situation drilling is done incrementally. In various cases, this method can provide access to a high gradient stress distribution because the residual stress in the material can be determined at each increment.

The major drawback of the non-destructive methods is that they do not give information for the distribution of global residual stresses in the composite or along the plies. The destructive and semi destructive techniques, which are also known as mechanical method, are dependent on deducing the original stress from the displacement acquired by completely or partially relieving the stress by removing material. These methods depend on the measurement of deformations due to the release of residual stresses upon removal of material from the specimen. The techniques which can measure the distribution of residual stresses are based mainly on destructive and semi destructive techniques [17]. These methods include: first ply failure, sectioning, contour, layer removal method, the incremental hole drilling method, the deep hole method, the Sachs Method and the crack compliance method.

2.6.1 First ply failure

The thermal contraction in symmetric cross-ply composites causes the development of tensile residual stresses in the transverse (90°) plies. This technique relies on measuring the difference between the apparent transverse tensile strength of unidirectional material and the stress required to initiate transverse cracking when the same material is embedded in a cross-ply laminate. When the composite material is loaded in the transverse direction, its tensile strength $\sigma_{0/90}^t$ (where t represents the transverse direction) has been found to be lower than the tensile strength of a similar unidirectional composite in the longitudinal (0°) direction $\sigma_{0/0}^l$ (where l presents the longitudinal direction). The tensile strength is calculated through acoustic emission of the first crack and therefore the term first ply failure comes up. The difference between the tensile strengths provides an approximation of the residual stresses between plies (interlaminar residual stresses) σ_R , where $\sigma_R = \sigma_{0/0} - \sigma_{0/90}^t$. The 90° plies are positioned at the external surface to ensure the noise of the cracking would not be suppressed [18].

2.6.2 Hole-drilling technique

The hole-drilling method is relatively straightforward and rapid; it is one of the most commonly used semi destructive methods of residual stress evaluation which can provide the measurement of residual stress distribution across the thickness in magnitude, direction and sense. It has the advantages of good precision, dependability and standardized test procedures, and suitable practical implementation. The principle involves introduction of a small hole (of about 1.8 mm diameter and up to about 2.0 mm deep) at the location where residual stresses are to be measured. The damage suffered by the specimen is restricted to the small, drilled hole, and is often tolerable or repairable. When the hole is drilled in the material locked up residual stresses are relieved and the corresponding strains on the surface are measured using suitable strain gauges bonded around the hole on the surface [19]. From the strains measured around the hole, the residual stresses are calculated using appropriate calibration coefficients derived for the particular type of strain gauge rosette used as well as the most suitable analysis procedure for the type of stresses expected [20].

The method is briefly summarized in six steps as follows:

- A special three or six strain gauge rosette is mounted on the test part at the point where residual stresses are to be determined.
- The gauge grips are wired and connected to a multi-channel static strain indicator.
- A precision milling is attached to the test part and correctly centered over a drill target on the rosette.
- A small, shallow hole is drilled through the geometric center of the rosette, after the zero balancing of the gauge circuit.
- Readings of the relaxed strains are then made which correspond to the initial residual stress.
- Using the special data-reduction relationship, the principal residual stresses and their angular orientation are calculated from the measured strain.

By reducing the respective depth of each increment, the sensitivity of the method for determining the residual stress profile in the through-depth of the material can be increased. Furthermore, it was found out that the relative gauge position plays a significant role in the quality and sensitivity of the residual stress calculations. It appears from the data tested that the best results are obtained for the $0.30 < \delta < 0.50$ range of values. The residual stress calculated cannot be used outside this range. Also the λ ratio does not have any significant influence, which implies that the geometry of the gauge does not play an important role in the range of strain gauge lengths studied. The variables δ and λ (Figure 2.3) are defined as follows:

- δ is the ratio of the hole radius to the radius of the inside of the strain gauge ($\delta = \frac{R_t}{R_{xj}}$)
- λ is the ratio of the hole radius to the radius of the middle of the strain gauge ($\lambda = \frac{R_t}{R_{xj}}$) [21].

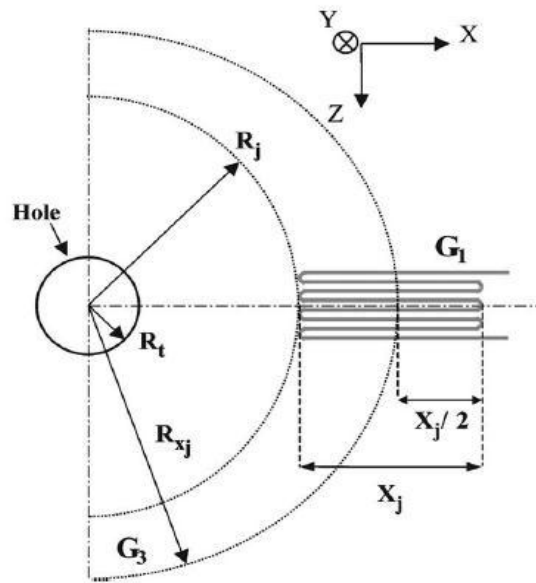


Figure 2.3 Relative locations of the hole and the strain (figure from [21])

The hole drilling method, as an experimental technique for measuring residual stresses, was proposed by Mathar in 1934, based on the work of Kirsch on the strain and stress distribution around through holes in thin plates (plane stress states) [46]. The technique evolved since then and in the 80's the American standard ASTM E837 standardized the technique [33]. However, the standard procedure only covered the case of uniform residual stresses through the depth. Due to the researches essentially developed in the 80's, the technique evolved to the determination of non-uniform residual stresses through the evaluation depth. For this, the hole has to be made step by step, i.e., incrementally. Finally in 2008 a new version of the American standard proposed for the first time a standard procedure for the determination of in-depth non uniform residual stresses, the so-called incremental hole-drilling technique. However, since the method implies the relation between the stresses existing at different depths with the released strains measured at surface, the method needs to be calibrated. Therefore a set of calibration coefficients must previously be experimentally or numerically determined, depending on the calculation method adopted. According to the American standard, the most correct calculation method, necessary to relate the measured strains with the existing residual stresses, is the so-called integral method, for which the related calibration coefficients can only be numerically determined by the finite element method.

Since then, the incremental hole-drilling technique is one of the most widely used techniques for measuring residual stresses. It is comparatively simple, cheap, quick and versatile. Apparatus can be

laboratory-based or portable, and the technique can be applied to a broad range of materials and components. This method was originally developed to measure residual stresses in isotropic or homogeneous materials and will be studied in detail in this work regarding its application to composite laminates.

2.6.3 Ring Core method

The ring-core method is an “inside-out” alternative of the hole-drilling method. While the hole-drilling method involves drilling a hole at the middle of the material and measuring the resulting deformation of the surrounding surface, the ring core (RC) technique [22, 23] involves cutting an annular groove into a component and the resulting surface strain relaxation within the central core is measured at predetermined depth increments using a strain gauge rosette or optical methods. As with the hole-drilling method, the ring-core method has a basic implementation to evaluate in-plane stresses [23], and an incremental implementation to determine the stress profile. The ring-core method has the advantage over the hole-drilling method that it provides much larger surface strains. However, is less frequently used because it creates much greater specimen damage and is much less convenient to implement in practice. In the past the RC technique was mainly used to measure ‘uniform’ stress profiles to a depth of 5mm or less, however with recent advancements in analysis techniques and the development of a core removal procedure these depths have been extended to 25mm [24].

2.6.4 The slitting method or crack compliance method

The slitting method is very similar to the hole-drilling method, but in this case a long slit rather than a hole is applied. Strain gauges are attached either on the front or back surfaces, or both, and the relieved strains are measured as the slit is incrementally increased in depth. The slit can be introduced by a thin saw, milling cutter [25 – 27]. Due to this, the residual stresses perpendicular to the cut can then be determined from the measured strains using finite element calculated calibration constants, in the same way as for hole-drilling calculations. In general, the slitting method has the advantage over the hole-drilling method in that it can evaluate the stress profile over the whole specimen depth, the surface strain gauge providing data for the near surface stresses, and the back strain gauge providing

data for the deeper stresses. The slitting method offers only the residual stresses normal to the cut surface, whereas the hole-drilling method provides all three in-plane stresses.

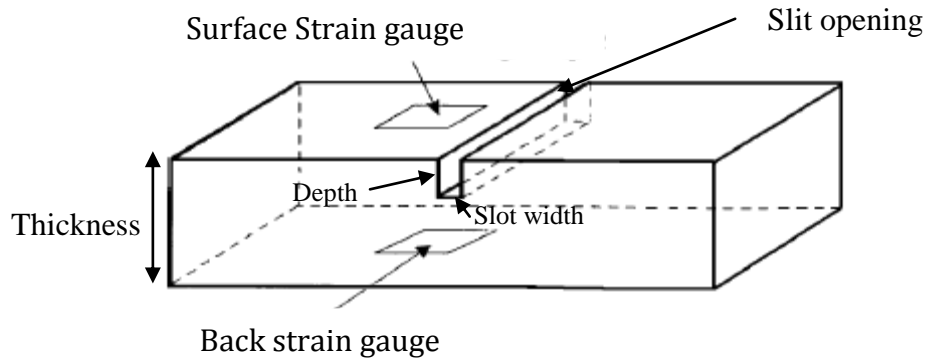


Figure 2.4 schematic diagram of the slitting method

2.6.5 Layer removal method

The layer removal method employs the taking away of thin layers of material from one surface of a plate. In this method, abrasion or milling is employed to remove one or more plies of the composite material. The inner stresses that are initially present in this layer are consequently eliminated and the plate therefore curves to re-establish force equilibrium. By measuring the strain and curvature of the laminate as successive layers are removed, it becomes possible to derive the stress profile through the original laminate. The layers removal from the composite material can be achieved by machining processes [28] splitting with a knife or by placing separation films within a laminate during cure when applied to composite laminates. In the layer removal method, abrasion or milling is employed to remove one or more plies of the composite material. The stresses released can be calculated through the measurement of the strains and the deformation which develops in the laminate after the material removal. Therefore, strain gauges are installed on the opposite side of the material removed, while the deformation can be measured by Moiré interferometry [18].

2.6.6 Deep hole method

The deep hole method [29] is a further alternative procedure that combines elements of both the hole-drilling and ring-core methods. A hole is first drilled through the thickness of the component, in this method. The diameter of the hole is measured accurately and then a core of material around the hole

is trepanned out, relaxing the residual stresses in the core. The diameter of the hole is re-measured allowing finally the residual stresses to be calculated from the change in diameter of the hole. The deep hole method is classified as a semi destructive method of residual stresses measurement since though a hole is left in the component, the diameter of the hole can be fairly small and could match with a hole that needs to be machined subsequently. The main feature of the method is that it enables the measurement of deep interior stresses. The deep-hole method bases its formulation on a calculation of the distortion of a hole in a plate subjected to loading. The method is particularly suited to thick components. Some investigators [30] have developed an extension to the method to allow the measurement of residual stress in orthotropic materials such as thick laminated composite components.

2.6.7 Sachs Method

This method is named after the inventor; Sachs [31] who developed a technique for the measurement of axisymmetric residual stresses from the analysis of strain relaxations during the incremental removal of layers of material from an axisymmetric component. He developed easier equations for finding the axisymmetric residual stresses in cylinder, and was the first to carry out the experimental procedure. The method is very similar to the layer removal method except that it is applied to rods and tubes rather than plates. Clearly the positioning of strain gauges on the inner surface of a component is only applicable to tubes or other hollow components. The technique allows axial, circumferential and radial residual stresses to be determined. Sachs method involves progressively removing “tubes” of material from the centre of a circular section. The residual stresses inside this material are released and the remaining material responds elastically, as each radial increment is removed. The response is typically measured using strain gauges aligned axially and circumferentially on the outer surface of the section. A deviation of the method allows for removal of material from the outer surface of tubes.

The material removal process is carried out from the opposite face to that end where the strain gauges are on and incrementally stepped towards the strain gauged surface. If the strain gauges are on the outer diameter of a cylinder, layers are removed from the inner diameter outwards. Each increment in machining removes an axisymmetric layer from the component until no more strain relaxation is

recorded. The resolution of the residual stresses measured, and hence the stress gradients, is dictated by the number of increments in material removal.

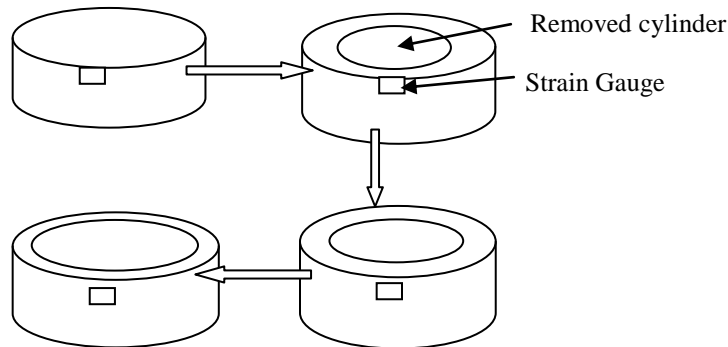


Figure 2.5 a schematic diagram of the Sachs Method

2.7. The incremental hole-drilling technique and its application to composite laminates

2.7.1 Introduction

The principle of this method is based on the stresses released by drilling, step by step, a small hole on the component containing residual stresses. The sizes of the hole and its geometry are changed due to the release of the stresses, since a portion of the material would be removed. These changes would result in deformation of the material surrounding the hole, relative to the uninterrupted location. The deformations are measured with a strain gauge rosette. The hole is drilled at the centre of the strain gauge rosette, which is bonded on the surface of the composite material. The so-called integral method, which was originally developed for isotropic and homogeneous materials, can be modified to accommodate the orthotropic and layered material behavior, such as it happens in carbon fibre reinforced polymers (CFRP), if proper calibration coefficients are introduced. These coefficients can be attained by numerical calculation.

Residual stresses are not constant, in composite materials, through the plies. In other words residual stresses are not uniform through the thickness of the composite. Hence, the modification of the hole drilling method is necessary to cater for non-homogeneity of the stress distribution through the thickness of a composite material such as CFRP. The basic principle for the calculation of stresses is the same with the hole drilling method, but in this case drilling is performed incrementally.

MATLAB scripts will be developed to process the measured strains and the stresses present before the hole-drilling activities.

The drilling technique is carried out according to the ASTM E837 standard (“Standard Test Method for Determining Residual Stresses by the Hole-Drilling Strain-Gauge Method”). Again, since the distances between the strain gauges and the hole are small, the drilling has to be performed without significant plastic deformations and heating. Therefore, high speed drilling machines of 300.000 revolutions per minute are used or air abrasive particles are used [32] – see Figure 2.6.

The influence of the depth increment in relation to the ply thickness and the relative position of the strain gauge are examined for the determination of residual stresses in composite laminates. Choosing an increment that is too significant (for example one increment per ply) can lead to slight overestimation of the residual stresses. This overestimation is caused by a too significant stresses relaxation during and after the drilling. Indeed the larger the increment depth, the longer the drilling time and in this case it becomes possible that a damage will appear as microscopic cracks and would lead to a stress relaxation which comes over the residual stresses relaxation. By reducing the respective depth of each increment, the sensitivity of the method for determining the residual stress profile in the through-depth of the material can be increased. Furthermore, it was found out that the relative gauge position plays a significant role in the quality and sensitivity of the residual stress calculations. It appears from the data tested that the best results are obtained.

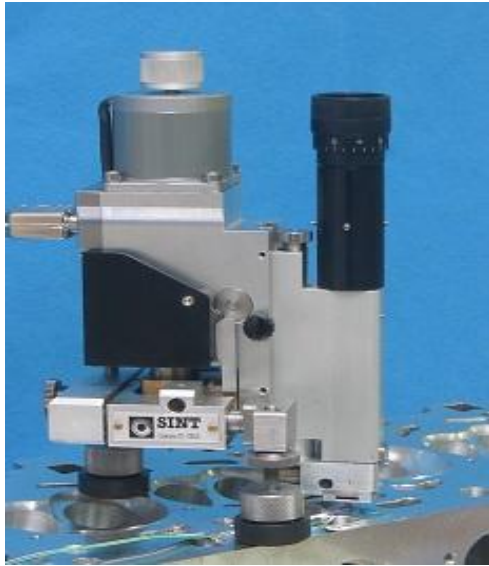


Figure 2.6 Incremental hole-drilling technique instruments use for the determination of residual stresses in carbon fibre reinforced polymer: SINT MTS3000 (left) and Vishay MS200 milling guide (right).

This method has been chosen for this research, principally for the following two reasons. Firstly, it can offer accurate results for the distribution of residual stresses through the thickness of a composite material. Secondly, the necessary apparatus are available, the MATLAB software to be used is accessible, and the strain gauges and drill-bits required are easy to obtain.

2.7.2 Strain gauge rosettes

They are instruments for measuring the normal strains or relieved strains along different directions in the essential surface of the test part of the material. To measure the relieved strains three resistance strain gauges in the form of rosette are mounted around the site of the hole before drilling is initiated.

The three rosette strain gauges are radially oriented and located with their centres at the radius R from the centre of the hole location. The angles between the gauges can be arbitrary chosen, but must be known, a 45-degree angular increment leads to simplest analytical expressions and consequently has become the standard for commercial residual stress rosettes.

It is imperative to note that when using strain gauges the numbering of the angles is done in the clockwise direction. It is to ensure that the angles from the principal axis are consistent for all measurements. There are numerous strain gauge rosettes which are used for determination of uniform stress and non-uniform stress which are described in the standard ASTM E -837-08. This deals with the evaluation of both constant and non-constant residual stress field through the thickness of the specimen rosettes indicated as A,B and C. in figure 2.6 [33].

Figure 2.7 shows a variety of residual stress strain gauge rosettes geometries currently existing. Type A, strain gauge is the most commonly used design gauge and is recommended for general purpose measurements. Type B is practical where measurements need to be made near a material or close to a fillet or radius. Type C gauge, which uses 6 grids, has been introduced lately to give improved strain sensitivity measurement.

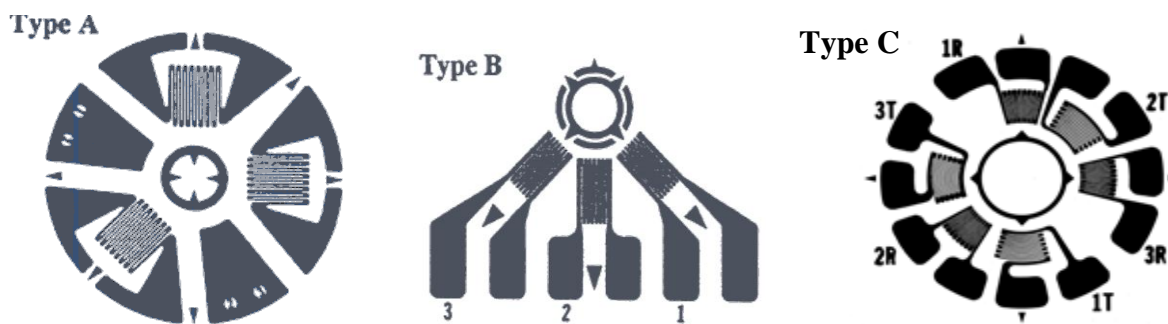


Figure 2.7 Three strain gauges rosettes existing in the ASTM E837-08 [33].

2.7.3 Residual stress evaluation procedures for orthotropic/anisotropic layered material

The hole-drilling method (HDM) is a well-established popular technique for measuring residual stresses in a wide range of engineering materials. From the point-of-view of Schajer and Yang [34], the existing hole-drilling method for stress-calculation adapted from the isotropic case was shown not to be suitable for orthotropic materials. A new stress-calculation method was depicted, based on the analytical solution for the displacement field around a hole in a stressed orthotropic plate. The validity of the method was assessed through a series of experimental measurements. It was established that in-depth non uniform residual stresses in many modern materials, such as fibre reinforced composites, which have distinctly anisotropic elastic properties, could not be determined

by the hole-drilling method. Schajer and Yang indicated that Bert et al. [35, 36] and Prasad et al. [37] generalized the computational procedure for the hole-drilling method for isotropic materials to extend the use of the method to orthotropic materials, however, the generalization was found not to be completely valid and final measurement error will depend on the orthotropic ratio (E_L/E_T). A different solution method that could be used for materials of any degree of elastic orthotropy was adapted, being however restricted to the case of in-depth uniform stresses. A Mathematical solution, based on the Classic Theory of Composites, was then proposed to determine the relationship between the residual stresses and the hole-drilling relieved strains around the hole in a stressed orthotropic plate [34].

Following the works of Bert et al. [35, 36] and Prasad et al. [37], Cherouat et al. [2] used a model to determine the distribution of residual stresses in laminates. The model is based on the following: the material is elastic and orthotropic, the components of stress in planes perpendicular to the surface are very small and strains on the surface are measured in three radial directions. The radial strains corresponding to the principal residual stresses of each ply at a number of increments are functions of the calibration coefficients. These coefficients can only be determined by using finite element analysis.

Sicot et al [3] highlighted on the previous findings that the (HDM) was originally established for isotropic and homogeneous materials for determination of the uniform residual stresses and the generalization based on Kirsh solution for its application to composite laminates must be better studied. In particular the final errors on the determined residual stresses. Despite these limitations, Sicot et al. [3] improved the work of Cherouat et al. [2], describing a numerical method for the determination of the necessary calibration coefficients for the application of the incremental hole-drilling technique to carbon/epoxy composite laminates.

The model used to evaluate the residual stress distribution was centered on the following assumptions;

1. The material was elastic and orthotropic and the stress component σ_{zz} perpendicular the surface of the material is very small.

2. The adopted model to describe the relation between the stress state and the strains on the surface corresponds to an adaptation of the model developed by Soete [38] for isotropic materials.

Sicot further asserted that Lake [39] suggested an introduction of a third coefficient with the aim of applying it to the case of orthotropic materials. The model was adapted to take into account the incremental character of the method and the relocation of the stresses after each increment. With the characteristic of the incremental method, the residual stresses in all the depth of the anisotropic material can be determined. The determination of the residual stresses requires the calculation of many coefficients of calibration, as stated before, and will be reviewed in detail further in this work.

The adopted theoretical approach, followed in this work, to determining the residual stresses from the measured strains are based on the method proposed by Cherouat et al. [2] and Sicot et al. [3, 5]. The procedure was also used in reference [40] and is currently being employed for the estimation of the residual stresses from the strains measured during experimental studies. This theoretical approach is described in the following.

The normal practice for measuring the relieved strains is to mount three resistance strain gauges in the form of rosette around the area where the hole is to be drilled, as indicated in figure 2.8.

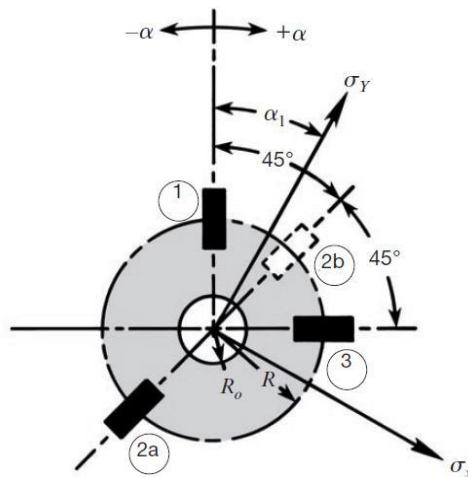


Figure 2.8 Strain gauge rosette arrangement placed around where the hole was to be drilled for determining residual stress [41]

Where:

α_1 = the acute angle from the nearer principal axis to gauge number 1.

$\alpha_2 = \alpha_1 + 45^\circ$ and $\alpha_3 = \alpha_1 + 90^\circ$

R_o = hole radius

R = radius of the strain gauge rosette in respect of the hole centre.

The change in strain at any location, for a fixed radial distance from the centre of the hole, can be described by the following relationship [5]:

$$\varepsilon_{in}(\theta_i) = A_{in}(\sigma_{1hi} + \sigma_{2hi}) + (\sigma_{1hi} - \sigma_{2hi})(B_{in} \cos 2\theta_i + C_{in} \sin 2\theta_i) \quad (1)$$

Where:

ε_{in} – is the strain contribution of layer i to the total strain measured on the surface for the n th increment;

σ_{1hi} and σ_{2hi} – are the main residual stresses in the layer i (the depth of the layer h_i);

θ_i – is the angle between the reference gauge and the first main direction of the residual stress;

A_{in} , B_{in} and C_{in} – are the calibration coefficients for the n th increment and loading for the i th layer.

The strain measurements in the three different directions are used to determine the three unknown factors σ_{1hi} , σ_{2hi} and θ_i for each drilling increment. When the first increment is drilled ($h_i=h_1$), the strain is obtained for the three different directions.

$$\varepsilon_{11}^1(\theta_i) = A_{11}(\sigma_{1h1} + \sigma_{2h1}) + (\sigma_{1h1} - \sigma_{2h1})(B_{11} \cos 2\theta_1 + C_{in} \sin 2\theta_1) \quad (2)$$

$$\varepsilon_{11}^2(\theta_i) = A_{11}(\sigma_{1h1} + \sigma_{2h1}) + (\sigma_{1h1} - \sigma_{2h1})(B_{11} \cos 2(\theta_1 + \alpha) + C_{in} \sin 2(\theta_1 + \alpha)) \quad (3)$$

$$\varepsilon_{11}^3(\theta_i) = A_{11}(\sigma_{1h1} + \sigma_{2h1}) + (\sigma_{1h1} - \sigma_{2h1})(B_{11} \cos 2(\theta_1 + \beta) + C_{in} \sin 2(\theta_1 + \beta)) \quad (4)$$

Where ε_{11}^1 is the combination in the j th direction and α and β are the angles of the 2nd and 3rd directions of increment.

After the n th increment process have been achieved the total depth becomes h_n and the equation becomes:

$$\varepsilon_{nn}^1(\theta_n) = A_{nn}(\sigma_{1hn} + \sigma_{2h1}) + (\sigma_{1h1} - \sigma_{2hi})(B_{nn} \cos 2\theta_n + C_{nn} \sin 2\theta_n) \quad (5)$$

$$\varepsilon_{nn}^2(\theta_n) = A_{nn}(\sigma_{1h1} + \sigma_{2h1}) + (\sigma_{1h1} - \sigma_{2hi})(B_{nn} \cos 2(\theta_n + \alpha) + C_{nn} \sin 2(\theta_n + \alpha)) \quad (6)$$

$$\varepsilon_{nn}^3(\theta_n) = A_{nn}(\sigma_{1h1} + \sigma_{2h1}) + (\sigma_{1h1} - \sigma_{2hi})(B_{nn} \cos 2(\theta_n + \beta) + C_{nn} \sin 2(\theta_n + \beta)) \quad (7)$$

After the first increment, the hole in the hole geometry is also taken into account. Each previously removed layer affects the total strain measured on the surface and the strain measured on the surface due to the removed layer only is expressed as follows ($\varepsilon_{nn}^j = \varepsilon_n^j$):

$$\varepsilon_n^1 = \varepsilon_{mn}^1 - \sum_{i=1}^{n-1} \varepsilon_{in}^1 \quad (a) \quad \varepsilon_n^2 = \varepsilon_{mn}^2 - \sum_{i=1}^{n-1} \varepsilon_{in}^2 \quad (b) \quad \varepsilon_n^3 = \varepsilon_{mn}^3 - \sum_{i=1}^{n-1} \varepsilon_{in}^3 \quad (c) \quad (8)$$

Where ε_{in}^j the contribution of the i layer in j direction in the case of the n th increment referring to equation (1), and ε_{mn}^j is the total strain measured on the surface by the strain gauge in j direction.

After 3 increments, for example, we obtain:

$$\varepsilon_3^1 = \varepsilon_{m3}^1 - \sum_{i=1}^2 \varepsilon_{i3}^1 = \varepsilon_{m3}^1 - (\varepsilon_{13}^1 + \varepsilon_{23}^1) \quad (9)$$

This gives:

$$\varepsilon_3^1 = \varepsilon_3^1 - [(A_{13}(\sigma_{1h1} + \sigma_{2h1}) + (\sigma_{1h1} - \sigma_{2h1})(B_{13} \cos 2\theta_1 + C_{13} \sin 2\theta_1)) + (A_{23}(\sigma_{1h2} + \sigma_{2h2}) + (\sigma_{1h2} - \sigma_{2h2})(B_{23} \cos 2\theta_2 + C_{23} \sin 2\theta_2))] \quad (10)$$

With this method, it is considered that, for each increment, the total strain measured on the surface can be broken down into two parts. The first part is due to the residual stress on the removed layer and the second part is the contribution residual stress redistribution caused by the change in geometry. When a 45° strain gauge rosette is used (0°, -135°, 90°), 3 equations are obtained for each drilling increment by reversing the system as follow:

$$\sigma_{1hn} = \frac{\varepsilon_n^1(A_{nn} - B_{nn} \sin 2\theta_n + C_{nn} \cos 2\theta_n) - \varepsilon_n^2(A_{nn} - B_{nn} \cos 2\theta_n - C_{nn} \sin 2\theta_n)}{2A_{nn}B_{nn}(-\sin \theta_n + \cos 2\theta_n) + 2A_{nn}C_{nn}(\sin 2\theta_n + \cos 2\theta_n)} \quad (11)$$

$$\sigma_{2hn} = \frac{-\varepsilon_n^1(A_{nn} - B_{nn} \sin 2\theta_n + C_{nn} \cos 2\theta_n) + \varepsilon_n^2(A_{nn} + B_{nn} \cos 2\theta_n - C_{nn} \sin 2\theta_n)}{2A_{nn}B_{nn}(-\sin \theta_n + \cos 2\theta_n) + 2A_{nn}C_{nn}(\sin 2\theta_n + \cos 2\theta_n)} \quad (12)$$

$$\theta_n = \frac{1}{2} \tan^{-1} \left[\frac{C_{nn}(\varepsilon_n^3 - \varepsilon_n^1) - B_{nn}(2\varepsilon_n^2 - \varepsilon_n^1 - \varepsilon_n^3)}{C_{nn}(\varepsilon_n^3 - \varepsilon_n^1 - \varepsilon_n^3) - B_{nn}(\varepsilon_n^3 - \varepsilon_n^1)} \right] \quad (13)$$

Equations 11, 12 and 13 are derived from equations 5, 6 and 7 for the principal residual stresses and their directions. The application of these equations to a real practical case affords the exact knowledge of the calibration coefficients A_{in} , B_{in} and C_{in} , which can only be numerically determined by finite element analysis, as it will be described in the following.

3. RESEARCH QUESTIONS/HYPOTHESIS

- Can the incremental hole-drilling technique (IHD) be reliably used for measuring residual stresses in composite laminates, such as carbon fibre reinforced polymers (CFRP)?
- What is the expected error on the residual stress determination using the selected theoretical approach for IHD residual stress determination?

4. RESEARCH AIMS AND OBJECTIVES

The main aim of this research work is to develop MATLAB scripts to determine residual stresses in carbon-fibre reinforced polymer composites using the incremental hole drilling technique (IHD). This is achieved through the following objectives:

- Establish a theoretical approach to relate the in-depth strain relaxation curves obtained during the incremental hole drilling technique and the residual stresses existing in a given CFRP sample, prior to the development of the MATLAB scripts (as per section 2.7.3).
- Develop a finite element analysis to determine the necessary calibration coefficients related with the selected theoretical approach defined previously. All residual stress calculation methods for the IHD technique imply the determination of specific calibration coefficients.
- Validate the theoretical approach and the developed MATLAB code through the assessment of experimental measurements previously performed by the research group [45]. This

validation uses in-depth strain relaxation curves previously obtained, which correspond to an in-depth uniform stress imposed during tensile tests (calibration tests) on selected CFRP specimens.

5. RESEARCH METHODS

5.1 Numerical Procedure

5.1.1 Introduction

For the implementation of the MATLAB scripts, for residual stress determination in composite laminates, based on the theoretical procedure described in section 2.7.3 and 5.1.2, specific calibration coefficients A_{in} , B_{in} , C_{in} must be determined numerically. These coefficients are material dependent for the case of orthotropic or anisotropic materials, as it happens with composite laminates. It means that they must be determined, case by case, depending on the composite laminate under study and the stacking sequence of its plies. It should be noted that, as stated in the ASTM E837-13 standard [33], these calibration coefficients can be considered independent of the material under testing for the case of isotropic materials. Therefore, the determination of residual stresses in composite laminates cannot be standardized as it is in the case of isotropic metallic materials in general. As explained in section 5.1.2, the finite element method is a suitable numerical method for this purpose.

Considering the experimental tests previously performed to this work, using the symmetric carbon fibre reinforced polymer (CFRP) composite with the stacking ply sequence $[0^\circ, 90^\circ]_{5s}$, which will be described in the following section 5.2, the finite element analysis was performed regarding the mechanical properties and specimens' geometry of this specific composite laminate. The finite element model was developed using APDL scripting for ANSYS and used to determine the specific calibration coefficients, which are necessary for residual stress calculation using the procedure described in section 2.7.3.

5.1.2 Determination of Calibration Coefficients

The approach followed in this work for the determination of the necessary calibration coefficients is described in detail in references [3, 5], for specific CFRP specimens. However, those calibration coefficients were not published by the authors. The calibration coefficients depend on the geometry of the hole, the strain gauge rosette and the relative position of layer i . It is impracticable to completely determine these coefficients experimentally. Three dimensional finite elements modeling were used by Sicot et al. [3, 5] to determine these coefficients. The unknown calibration coefficients A_{in} , B_{in} , C_{in} are determined by finite element analysis which simulates the incremental hole drilling procedure. For the calculation of the A_{in} calibration coefficients, a uniform stress (uniform pressure) should be applied at the hole boundaries of each increment in the finite element model. The coefficients A_{in} can be determined by applying an equilibibaxial residual stress field, which is equivalent to uniform pressure of $p = \sigma_{1i} = \sigma_{2i} = \sigma$, acting on the inside surface of the hole. The finite element model was used to obtain the radial displacement U_{in} on the surface. The coefficient A_{in} was then calculated by the following equation [3, 5]:

$$A_{in} = \frac{U_{in}(r_2,0) - U_{in}(r_1,0)}{2\sigma L} \quad (14)$$

Where: $L = r_2 - r_1 = \text{gauge length}$

The composite laminates were modeled using 3D orthotropic finite elements of the (C3D8) type in ABAQUS/standard in references [3, 5]. Because of the axial symmetry of the geometry, the loading and the mechanical properties, only a quarter of the laminated structure was modeled (Figure 2.9).

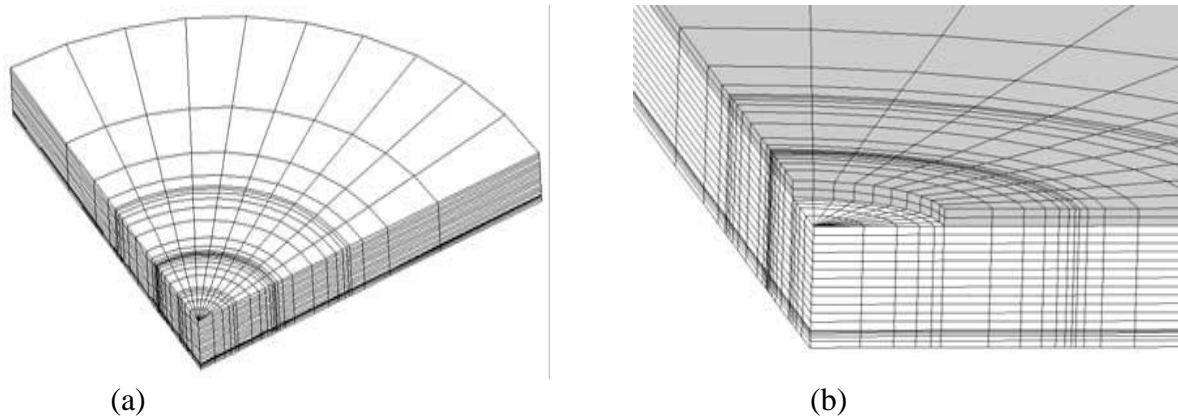


Figure 5.1 Finite element models after the first increment [3].

For fifth stage in the incremental hole drilling, the coefficients A_{15} , A_{25} , A_{35} , A_{45} and A_{55} can be determined. Figure 5.2 depicts the steps in carrying out incremental drilling in 5 stages.

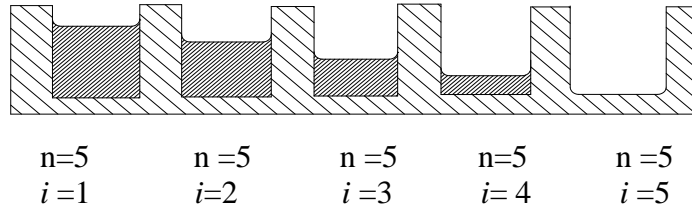


Figure 5.2 Fifth drilling stage.

Likewise, the coefficients B_{in} and C_{in} can be determined by imposing a pure shear stress field, as follows:

$\sigma_{1i} = -\sigma_{2i} = \sigma$, acting on inside surface of the hole, in each direction.

$$B_{in} = \frac{U_{in}(r_2, 0) - U_{in}(r_1, 0)}{2\sigma L} \quad C_{in} = \frac{U_{in}\left(r_2, \frac{\pi}{4}\right) - U_{in}\left(r_1, \frac{\pi}{4}\right)}{2\sigma L} \quad (15)$$

Following the determination of each coefficient, the residual stress can be calculated using equations (11) and (12). In the case of a standard laminate and pre-determined experimental geometric parameters, that is; length of strain gauge, hole diameter, depth of each increment, etc, the calibration coefficients have to be computed one at a time. In this situation, it is only the strain which occurs after drilling is measured for each test.

5.2 Material and Experimental Procedure

5.2.1 Material and specimens

For the validation of the residual stress calculation procedure implemented using MATLAB, regarding the application of the incremental hole-drilling technique to composite laminates, a carbon-fibre reinforced material (CFRP), which was previously used in another study, was selected. These CFRP specimens were made in carbon/epoxy prepreg [42], which were cured in autoclave at 180 °C. The stacking sequence is $[0^\circ/90^\circ]_{5s}$ for a total 2 mm thickness. That means 20 layers of carbon/epoxy

prepreg with an individual thickness of about 100 μm in a symmetric formation. The prepreg used was M18/M55J from Hexcel.

The mechanical properties of the carbon/epoxy lamina had been taken from a previous work [43] and are listed in Table 5.1. The properties are taken from a work of a curved beam test structure in carbon/epoxy using Bragg sensors and are essential for the finite element analysis carried out in this work and for validation of the MATLAB scripts developed.

Table 5.1 Properties of the material used in the test [43]

Description		Units
Fibre direction modulus of elasticity (E_{11})	300000	MPa
Transverse to fibre modulus of elasticity (E_{22})	6300	MPa
Through thickness modulus of elasticity (E_{33})	6300	MPa
In-plane shear modulus in the fibre direction (G_{12})	4300	MPa
In-plane shear modulus in the transverse to fibre direction (G_{23})	2300	MPa
In-plane shear modulus in the through thickness direction (G_{13})	4300	MPa
Poisson ratio in the direction of the fibre ($\nu_{12} = \nu_{13}$)	0.32	-
Poisson ratio in the transverse to fibre ($\nu_{23} = \nu_{32}$)	0.38	-
Poisson's ration in the through thickness ($\nu_{21} = \nu_{31}$)	0.002	-

5.2.2 Brief description of the experimental procedure used for validation purposes

A method developed by Nobre et al. [16] was used for validation purposes of the MATLAB scripts developed in this work, for the residual stress evaluation by the modified integral method in orthotropic materials. The proposed method was developed to quantify the effect of the drilling process on the material by determining the induced drilling strains. For this, the initial residual stresses existing in the studied composite laminate, which was described in the previous section, had to be eliminated. This way, the final in-depth strain relaxation curves obtained during these experimental tests, are referred to a specific uniaxial and uniform stress. These curves are further used as input of the MATLAB scripts developed by validation purposes.

Figure 5.3 below shows how applied uniaxial stresses can eliminate the effect of the initial residual stresses, existing in the material before drilling. Based on the superposition principle, a differential calibration stress instead of an absolute stress is considered. Thus, the methodology is valid for any

material that behaves linearly and elastically. In the case of its application to the composite laminates, however, the diameter of the hole should be much larger than the reinforcing fibre filaments to ensure that homogeneous stresses are applied. Mathematically, the principle to eliminate the initial residual stress can be explained as follows: if σ_{RS} is the initial residual stress and σ_{Ical} a stress generated, corresponding to a given applied axial load F_I , the final stress will be σ_I , given by:

$$\sigma_I = \sigma_{RS} + \sigma_{Ical} \quad (16)$$

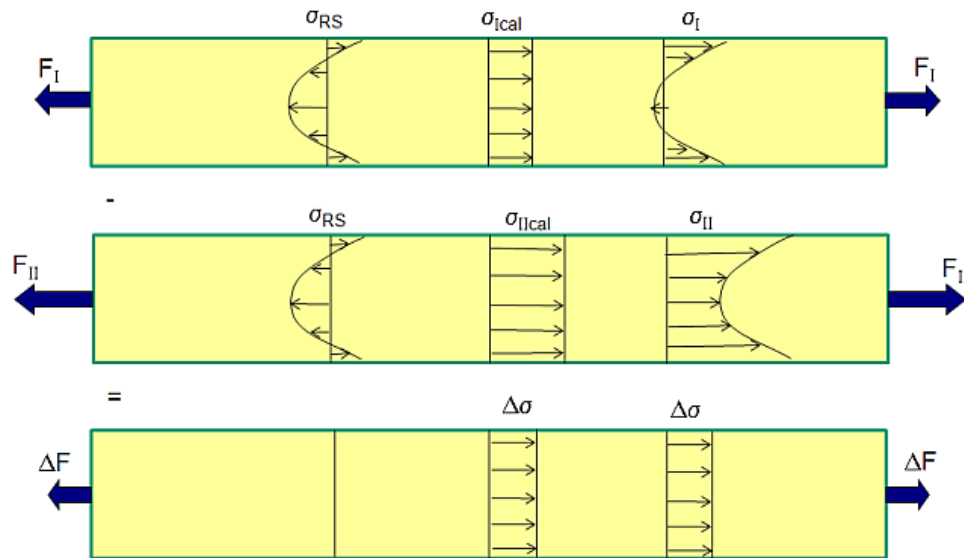


Figure 5.3 Superposition principle to eliminate the initial residual stresses.

Increasing the applied load to F_{II} , if the material behaves elastically, the σ_{RS} remains unchanged and it is also possible to write:

$$\sigma_{II} = \sigma_{RS} + \sigma_{IIcal} \quad (17)$$

Obviously, σ_{II} , when F_{II} is applied, should be kept below a maximum value to avoid any damage around the hole, due to the effect of the stress concentration induced by the hole itself. Therefore, for a pure elastic regime, the initial residual stress, σ_{RS} , remains unchanged. Taking the difference between equations (16) and (17), the effect of the initial residual stress is eliminated, i.e;

$$\sigma_{cal} = \Delta\sigma = \sigma_{IIcal} - \sigma_{Ical} = \sigma_{II} - \sigma_I \quad (18)$$

The calculation of the maximum load was made considering carbon epoxy lamina in longitudinal 0° direction, for the material and specimens described in section 5.1.1 above. Since the transverse tensile strength in the 90° ply is very low, it was decided to reduce the maximum applied load to $F_{II} = 5$ kN, avoiding fracture of the transverse fibres and delamination of the specimens used. The corresponding maximum applied stress was $\sigma_{II} = 94$ MPa.

To keep the specimen fixed after drilling each depth increment, as per Table 5.2, a minimum applied force, F_I , of around 1064 N was considered, which corresponds to a minimum applied stress of $\sigma_I = 20$ MPa. Therefore, the calibration stress to be considered is $\sigma_{cal} = 74$ MPa. The loading and unloading cycles during the calibration procedure are presented in Figure 5.4.

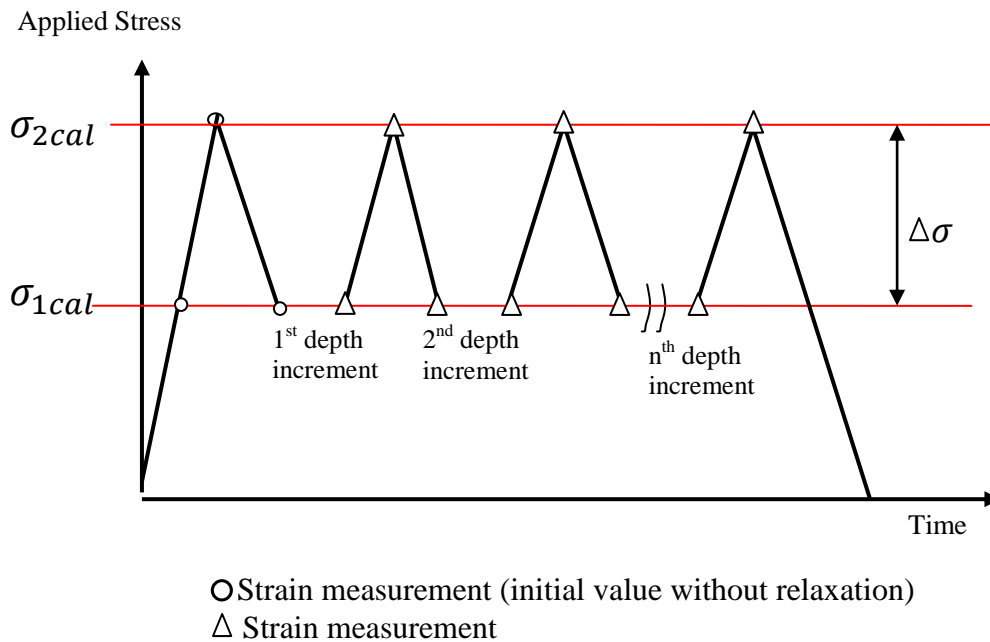


Figure 5.4 The schematic diagram of the Sequence of applied load cycles during the calibration procedure

The CFRP specimen was tensioned with around 500 N/min to a load $F_I = 1064$ N and a corresponding stress $\sigma_{Ical} = 20$ MPa, which hold the specimen in an aligned position as well. The

specimen is then loaded until the maximum load $F_{II} = 5000$ N and a corresponding stress $\sigma_{IIcal} = 94$ MPa. The material was then unloaded to the minimum load F_I . The values of strain direction for ε_1 (0°) ε_2 (45°) and ε_3 (90°) were taken continuously during the loading and unloading cycles and recorded in the database. The obtained in-depth strain relaxation values are presented in table 6.1.

5.2.3 Incremental hole-drilling parameters

The incremental hole-drilling parameters used in the previous experimental work described in section 5.2.2 are as indicated in Table 5.2 below. The specimens used were subjected to the applied tensile stress of 74 MPa, and the incremental hole-drilling technique was applied to these specimens to evaluate the in-depth strain relaxation curves. The MATLAB script developed uses these curves as input and the corresponding output, i.e., the calculated stress, compared with the experimental stress applied (74 MPa), enabling a validation of this work.

Table 5.2 incremental hole-drilling parameters previously used during the tests [32, 43]

Description		Units
Increments per ply	2	
Total number of increments	20	
Depth per increment	0.05	mm
Applied tensile stress (calibration tests)	74	MPa
Total drilled hole depth	1.0	mm
Diameter of the drill bit	1.6	mm
Feed rate	$\ll 0.010$	mm/min
Cutting speed	1500	m/min
Rotation speed	300,000	rpm

An ASTM standard strain-gauge rosette was positioned on the surface of the CFRP specimen in order to measure the resulting strain relief. Figure 5.5 shows the coordinate system, the hole-geometry and the position of the strain-gauge.

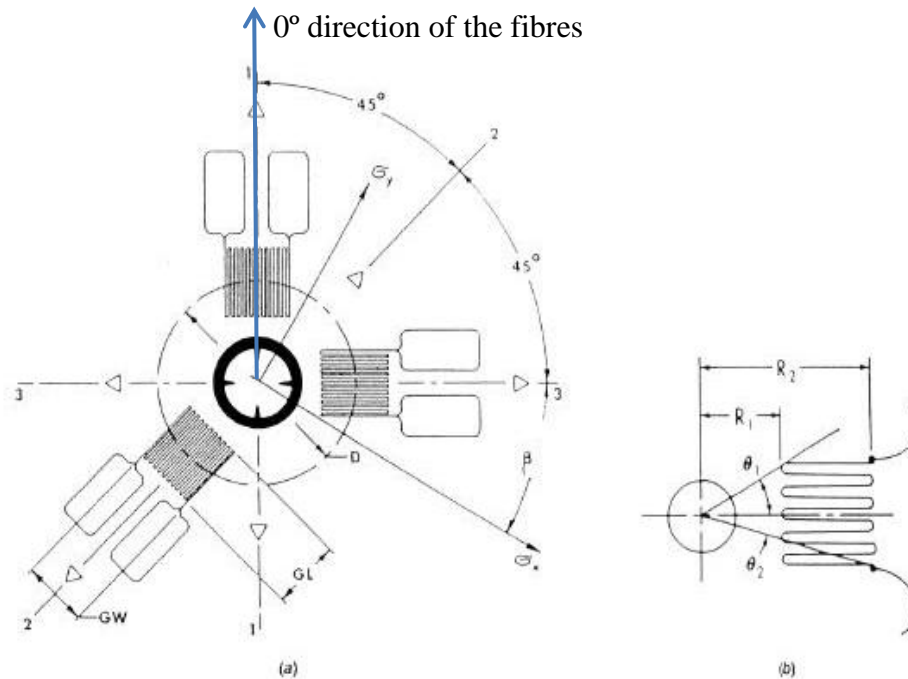


Figure 5.5 The coordinate system, the hole geometry and the position three-clockwise (CW) strain gauge rosette for the incremental hole-drilling method [25]

6. MATLAB SCRIPT DEVELOPMENT

A main target of this research was to develop scripts using MATLAB software to calculate residual stresses in orthotropic materials from series of strain relaxation previously determined using the incremental hole-drilling technique. A programme, therefore, was designed using MATLAB software to execute the calculation procedures to determine residual stresses in carbon fibre reinforced polymer (CFRP), according to the theoretical approach presented in section 2.7.3.

The development of the MATLAB scripts was based on equations 5, 6, 7 and 8, which were proposed by Sicot et al. [3]. The MATLAB code developed calculates the three unknown variables σ_{1hi} , σ_{2hi} and θ_i for each drilling increment. The experimental results of strain-depth relaxation obtained, and presented in the following in table 7.4, were used as input in the coded script to determine the unknown variables. When the first increment is drilled ($h_i=h_1$), the strain is obtained for the three different directions. The strain relaxations are determined as indicated in equations 8(a), 8(b) and 8(c) above, which are coded in the MATLAB script to calculate them. For example, after the third increment the equation for the determination of the strain relaxation, will be determined by:

$$\varepsilon_3^1 = \varepsilon_{m3}^1 - \sum_{i=1}^2 \varepsilon_{i3}^1 = \varepsilon_{m3}^1 - (\varepsilon_{13}^1 + \varepsilon_{23}^1)$$

Where:

the ε_3^1 is indicated in the MATLAB scripts as $e3 = \text{Emn3}(:,n) - \text{sum}(\text{Emn3}(:,1:1:n-1))$;

Emn3 = the strains measured from the strain gauge 3 in matrix Emn

e3 = the strain measured on the surface due to the removed layer only obtained from the third strain

The calibration coefficients, A_{nn} , B_{nn} and C_{nn} in equations (5), (6) and (7) in section 2.7.3 are represented in the MATLAB script as follows:

Amn = Matrix of calibration coefficients of A_{in}

Bmn = Matrix of calibration coefficients of B_{in}

Cmn = Matrix of calibration coefficients of C_{in}

The other variables used in the MATLAB scripts are explained as follows:

Depth = incremental distance downward in the material.

Emn = the matrix of the strains measured from the three strain gauges

Emn1 = the strains measured from the strain gauge 1 in matrix Emn

Emn2 = the strains measured from the strain gauge 2 in matrix Emn

Emn3 = the strains measured from the strain gauge 3 in matrix Emn

e1 = the strain measured on the surface only due to the removed layer only obtained from the first strain gauge from the incremental hole drilling.

e2 = the strain measured on the surface only due to the removed layer obtained from the second strain gauge from the incremental hole-drilling.

e3 = the strain measured on the surface only due to the removed layer only obtained from the third strain gauge from the incremental hole-drilling.

An = a single value of the calibration constant from Amn

Bn = a single value of the calibration constant from Bmn

Cn = a single value of the calibration constant from Cmn

Sigma1 = the uniform residual stress in the principal y-direction
 Sigma2 = the uniform residual stress in the principal x-direction
 theta = is the measured angle from the principal axis to the strain gauge 1 axis.
 e11, e22 and e33 = the plotted values of strain relaxation from the three rosette gauges.

The following MATLAB script calculates the strain relaxation in the direction of each strain gauge;

e1 = Emn1(:,n)-sum(Emn1(:,1:1:n-1)); calculates and records the strain relaxation in each incremental drill in the first rosette gauge until the nth increment.
 e2 = Emn2(:,n)-sum(Emn2(:,1:1:n-1)); calculates and records the strain relaxation in each incremental drill in the second rosette gauge until the nth increment.
 e3 = Emn3(:,n)-sum(Emn3(:,1:1:n-1)); calculates and records the strain relaxation in each incremental drill in the third rosette gauge until the nth increment.

The MATLAB script used to solve the numerical equations, from strain relaxation for each increment of hole drilled, to obtain the angle theta and the minimum and maximum stresses experienced by the material, can be seen below. The calibration coefficient matrices (Amn, Bmn and Cmn) must be previously determined, as it will be explained in section 7.1.

```
format short e
Amn=[-4.50E-08,-1.10E-06,-1.60E-06,-2.10E-06,-2.40E-06,-2.70E-08,-3.00E06,...
      -3.20E-06,-3.40E-06,-3.50E-06,-3.60E-06,-3.70E-06,-3.70E-06,-3.80E-06,...
      -3.80E-06,-3.80E-06,-3.80E-06,-3.90E-06,-3.90E-06,-3.90E-06];

Bmn=[1.67E-10,-9.20E-09,-1.20E-08,-1.50E-08,-1.70E-08,-1.80E-08,-2.00E-08,...
      -2.20E-08,-2.30E-08,-2.40E-08,-2.60E-08,-2.80E-08,-2.90E-08,-3.00E-08,...
      -3.20E-08,-3.30E-08,-3.40E-08,-3.50E-08,-3.60E-08,-3.70E-08];

Cmn=[6.33E-11,7.71E-09,-9.73E-09,9.79E-09,9.88E-09,9.63E-09,8.27E-09,...
      5.69E-09,4.44E-09,3.33E-09,1.38E-09,-1.30E-10,-2.80E-08,-3.50E-09,...
      -5.10E-09,-7.10E-09,-8.00E-09,-8.70E-09,-9.80E-09,-1.00E-08];

Depth = [0.0508,0.1016,0.1524,0.2032,0.2540,0.3048,0.3556,0.4064,0.4572,...
          0.5080,0.5588,0.6096,0.6604,0.7112,0.7620,0.8128,0.8636,0.9144,...
          0.9652,1.0160]';

Emn=[8,0,-11;-77,-4,-12;-83,-12,-10;-87,-20,-9;-126,-26,-6;-167,-30,-3;...
      -171,-36,-1;-174,-51,1;-188,-55,5;-202,-55,10;-205,-53,11;-206,-66,12;...
      -210,-61,16;-213,-64,20;-214,-77,21;-215,-77,21;-215,-81,25;-215,-85,29;...
      -216,-87,29;-216,-85,29];

Emn1 = Emn(:,1)';
Emn2 = Emn(:,2)';
Emn3 = Emn(:,3)';
```

```

for n = 1:20
    e1 = Emn1(:,n)-sum(Emn1(:,1:1:n-1));
    e2 = Emn2(:,n)-sum(Emn2(:,1:1:n-1));
    e3 = Emn3(:,n)-sum(Emn3(:,1:1:n-1));
    An = Amn(1,n);
    Bn = Bmn(1,n);
    Cn = Cmn(1,n);
    Theta = 0.5*atan((Cn*(e3-e1)-Bn*(2*e2-e1-e3))/(Cn*(2*e2-e1-e3)+Bn*(e3-e1)));
    Sigma1 = (e1*(An-Bn*sin(2*theta)+Cn*cos(2*theta))-e2*(An-Bn*cos(2*theta)-
    Cn*sin(2*theta))...
    /((2*An*Bn)*(sin(2*theta)+cos(2*theta))+(2*An*Cn)*(sin(2*theta)+cos(2*theta)));
    Sigma2=(e1*(An+Bn*sin(2*theta)+Cn*cos(2*theta))+e2*(An+Bn*cos(2*theta)+Cn*sin(2*theta)
    )).../((2*An*Bn)*(sin(2*theta)+cos(2*theta))+(2*An*Cn)*(sin(2*theta)+cos(2*theta)));
    disp([Sigma1,Sigma2])
end

```

Additional scripts to plot the results can be seen in Appendix A.

7. RESULTS AND DISCUSSION

7.1 Calibration coefficient matrices

Following the procedure already described in section 5.1.2, the finite element analysis was conducted twice, using two different stress states, to determine the calibration coefficients, according to equations (14) and (15), respectively. The numerical model was developed using ANSYS Parametric Design Language (APDL) for ANSYS 15.0. The model uses quadratic 20-node 3D layered solid elements SOLID186. Figures 7.1 and 7.2 show the three dimensional (3D) finite element mesh (FEM) used for the hole-drilling FEM simulation.

Two depth increments per ply in the $[0/90]_{5s}$ CFRP composite laminate were considered, which fits the experimental procedure previously performed. For this composite laminate, which mechanical properties and specimen geometry were described in section 5.1, it was only necessary to consider a $\frac{1}{4}$ model due to symmetry conditions.

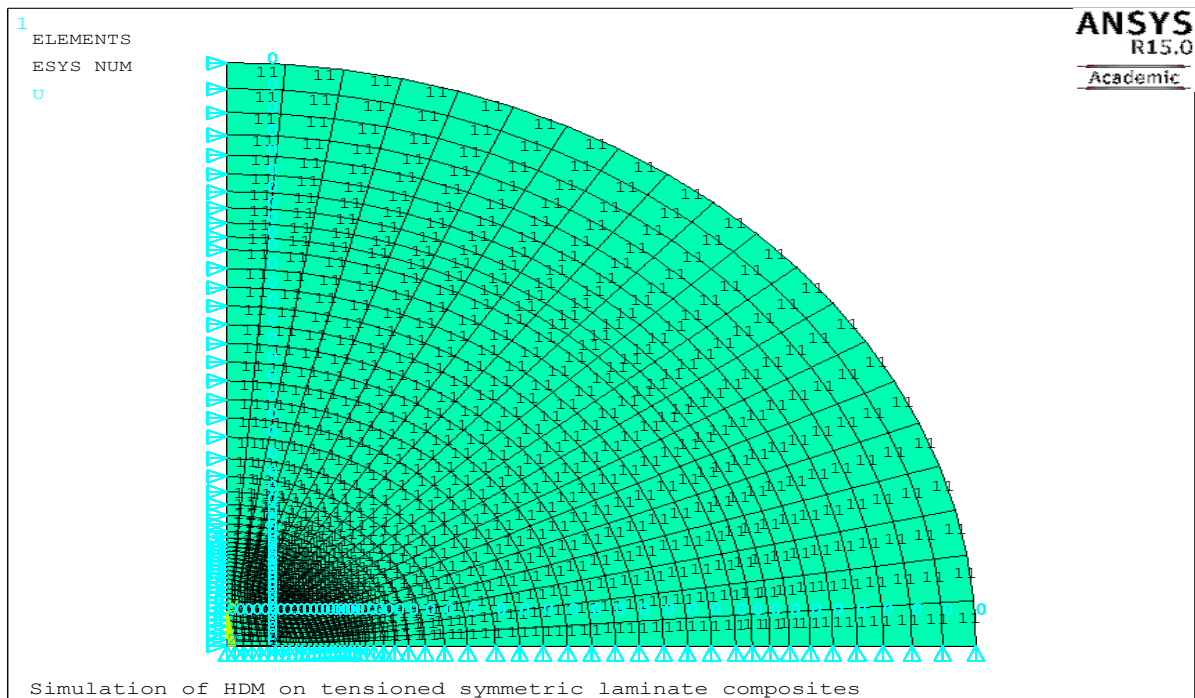


Figure 7.1 3D finite element mesh used in the FEM simulation of the $[0/90]_{5s}$ composite-laminate

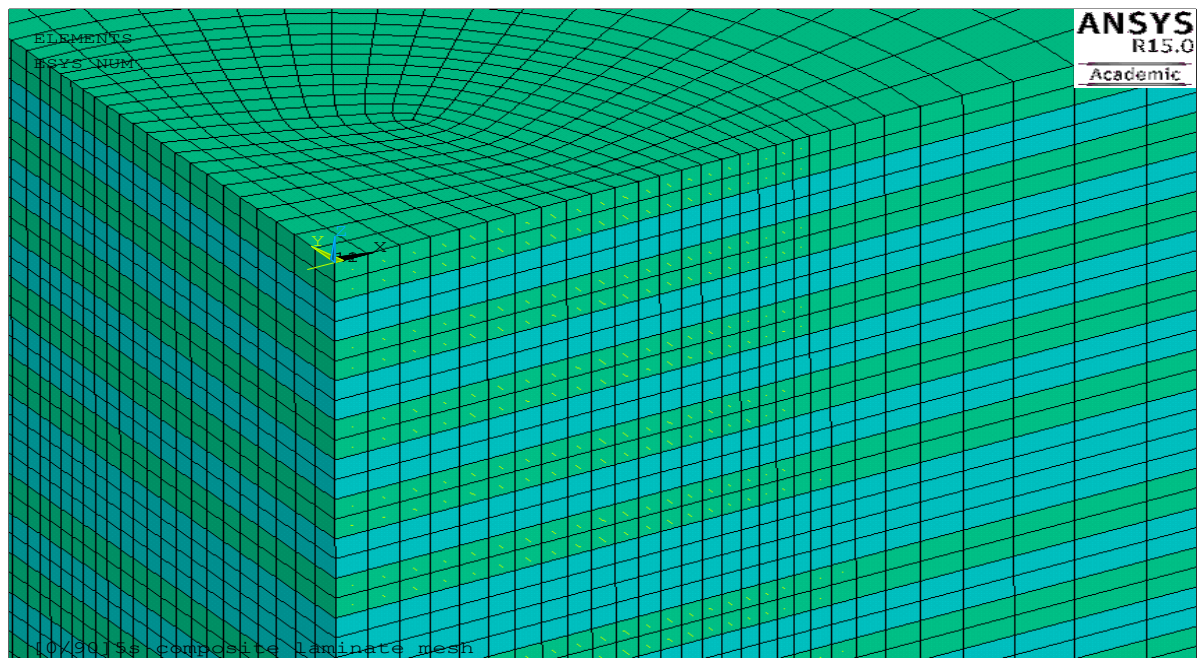


Figure 7.2 3D finite element mesh used in the hole-drilling FEM simulation of the $[0/90]_{5s}$ composite laminate (closer view) – two depth increments per ply were used.

For each depth increment considered, as per Table 5.2, two stress states were imposed to the hole surface in each depth increment, as explained in section 5.1.2 – see equations 14 and 15. However, to take into account the effect of the finite area of the strain gauges used during the experimental tests, the strain/nodal displacement values were integrated over the area corresponding to each strain-gauge grid. The relative size of the strain gauge used can be seen in Figure 7.3 – strain gauge grid oriented at 45°.

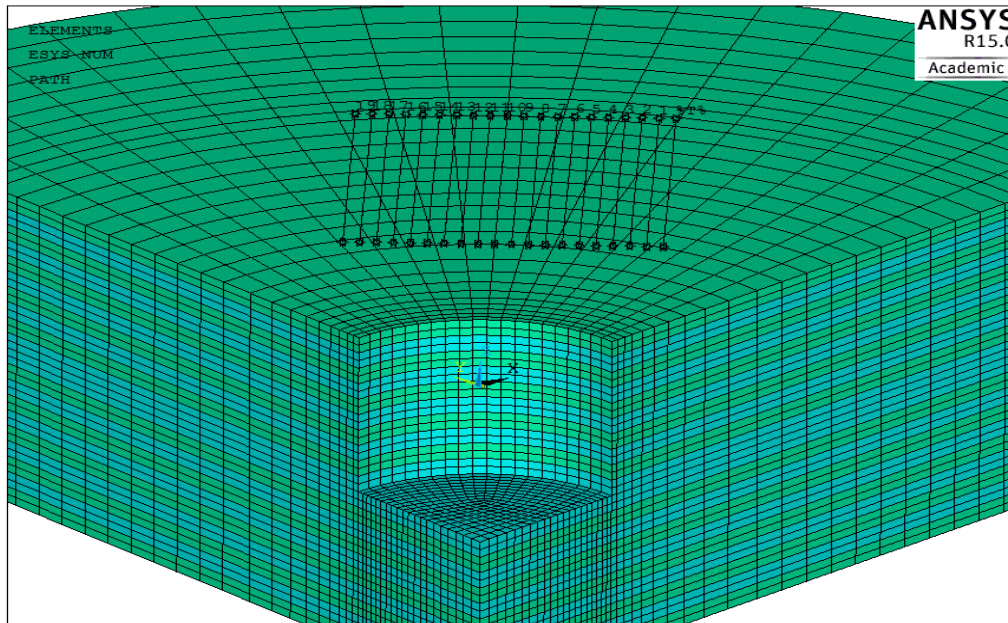


Figure 7.3 Relative size of the strain gauge area in the 3D finite element mesh used in the hole-drilling FEM simulation of the $[0/90]_{5s}$ composite laminate (1mm hole-depth).

As an example of the calculations performed, Fig. 7.4 shows the stress field (von Mises stress) and the corresponding strain field around the hole, corresponding to 1 mm hole depth during the determination of the constant A_{in} (last values of this matrix are shown in Table 5.4).

For the calculation of A_{in} , B_{in} and C_{in} , the calibration coefficient matrices, an unitary uniform stress (1 MPa) was applied at the hole boundaries of each depth increment performed in the finite element model. As mentioned before, two distinct stress states must be applied to the FEM model for the determination of A_{in} (hydrostatic stress state) and B_{in} and C_{in} (pure shear stress state).

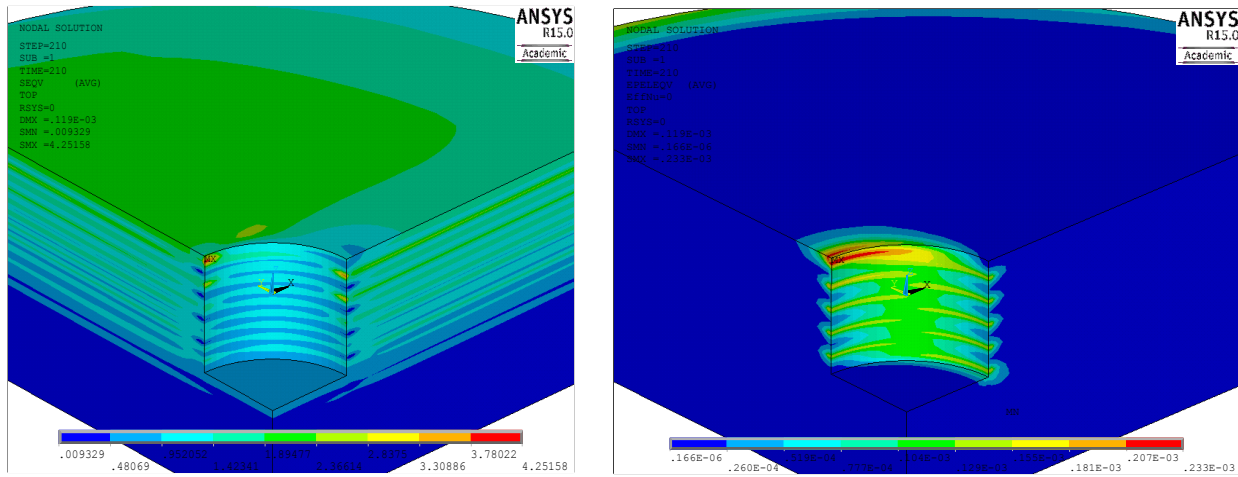


Figure 7.4 von Mises stress field (left) and strain field during the determination of the coefficient constants matrix A_{in} (1mm hole-depth)

Evoking equations 14 and 15, equations 16, 17 and 18 indicated below, were then used to calculate the coefficients corresponding to each depth increment, after the numerical determination by FEM of the displacement values U :

$$A_{in} = \frac{U_{in}(r_2, 0) - U_{in}(r_1, 0)}{2\sigma L} \quad (16)$$

$$B_{in} = \frac{U_{in}(r_2, 0) - U_{in}(r_1, 0)}{2\sigma L} \quad (17)$$

$$C_{in} = \frac{U_{in}\left(r_2, \frac{\pi}{4}\right) - U_{in}\left(r_1, \frac{\pi}{4}\right)}{2\sigma L} \quad (18)$$

In these equations r_2 , is the outside diameter of the rosette strain gauges, r_1 , the inner diameter of the rosette strain gauges, $L = r_2 - r_1$, is the gauge length, σ is the magnitude of the applied stress (unitary hydrostatic stress or pure shear stress, depending on the coefficients being determined), U_{in} is the radial displacement at surface.

The information collected from the FEM simulation was presented in the form of matrices. Three lower triangular matrices were obtained for A_{in} , B_{in} and C_{in} , as presented in Tables 7.1, 7.2 and 7.3. The simulations were performed to determine the displacements and these displacements are then

used to calculate the calibration coefficient values. The values obtained are recorded in a twenty by twenty matrix, as shown in Tables 7.1, 7.2 and 7.3.

Table 7.1 – Calibration coefficient matrix *A_{in}*

MATRIX A																			
-4.5E-08	0	0	0	0	0	0	0	0	0	0	0	0	0	0	0	0	0	0	0
-6.8E-08	-1.1E-06	0	0	0	0	0	0	0	0	0	0	0	0	0	0	0	0	0	0
-1.1E-06	-1.1E-06	-1.6E-06	0	0	0	0	0	0	0	0	0	0	0	0	0	0	0	0	0
-1.6E-06	-1.6E-06	-2.E-06	-2.E-06	0	0	0	0	0	0	0	0	0	0	0	0	0	0	0	0
-2.1E-06	-2.1E-06	-2.E-06	-2.E-06	-2.4E-06	0	0	0	0	0	0	0	0	0	0	0	0	0	0	0
-2.4E-06	-2.4E-06	-2.E-06	-2.E-06	-2.4E-06	-2.7E-08	0	0	0	0	0	0	0	0	0	0	0	0	0	0
-2.8E-06	-2.8E-06	-3.E-06	-3.E-06	-2.8E-06	-2.8E-06	-3.0E-06	0	0	0	0	0	0	0	0	0	0	0	0	0
-3.0E-06	-3.0E-06	-3.E-06	-3.E-06	-3.0E-06	-3.0E-06	-3.0E-06	-3.2E-06	0	0	0	0	0	0	0	0	0	0	0	0
-3.2E-06	-3.2E-06	-3.E-06	-3.E-06	-3.2E-06	-3.2E-06	-3.2E-06	-3.2E-06	-3.4E-06	0	0	0	0	0	0	0	0	0	0	0
-3.4E-06	-3.4E-06	-3.E-06	-3.E-06	-3.4E-06	-3.4E-06	-3.4E-06	-3.4E-06	-3.4E-06	-3.5E-06	0	0	0	0	0	0	0	0	0	0
-3.5E-06	-3.5E-06	-4.E-06	-4.E-06	-3.5E-06	-3.5E-06	-3.5E-06	-3.5E-06	-3.5E-06	-3.5E-06	-3.6E-06	0	0	0	0	0	0	0	0	0
-3.6E-06	-3.6E-06	-4.E-06	-4.E-06	-3.6E-06	-3.6E-06	-3.6E-06	-3.6E-06	-3.6E-06	-3.6E-06	-3.6E-06	-3.7E-06	0	0	0	0	0	0	0	0
-3.7E-06	-3.7E-06	-4.E-06	-4.E-06	-3.7E-06	-3.7E-06	-3.7E-06	-3.7E-06	-3.7E-06	-3.7E-06	-3.7E-06	-3.7E-06	-3.7E-06	-3.7E-06	0	0	0	0	0	0
-3.7E-06	-3.7E-06	-4.E-06	-4.E-06	-3.7E-06	-3.7E-06	-3.7E-06	-3.7E-06	-3.7E-06	-3.7E-06	-3.7E-06	-3.7E-06	-3.7E-06	-3.7E-06	-3.8E-06	0	0	0	0	0
-3.8E-06	-3.8E-06	-4.E-06	-4.E-06	-3.8E-06	-3.8E-06	-3.8E-06	-3.8E-06	-3.8E-06	-3.8E-06	-3.8E-06	-3.8E-06	-3.8E-06	-3.8E-06	-3.8E-06	-3.8E-06	0	0	0	0
-3.8E-06	-3.8E-06	-4.E-06	-4.E-06	-3.8E-06	-3.8E-06	-3.8E-06	-3.8E-06	-3.8E-06	-3.8E-06	-3.8E-06	-3.8E-06	-3.8E-06	-3.8E-06	-3.8E-06	-3.8E-06	-3.8E-06	0	0	0
-3.8E-06	-3.8E-06	-4.E-06	-4.E-06	-3.8E-06	-3.8E-06	-3.8E-06	-3.8E-06	-3.8E-06	-3.8E-06	-3.8E-06	-3.8E-06	-3.8E-06	-3.8E-06	-3.8E-06	-3.8E-06	-3.8E-06	-3.8E-06	0	0
-3.8E-06	-3.8E-06	-4.E-06	-4.E-06	-3.8E-06	-3.8E-06	-3.8E-06	-3.8E-06	-3.8E-06	-3.8E-06	-3.8E-06	-3.8E-06	-3.8E-06	-3.8E-06	-3.8E-06	-3.8E-06	-3.8E-06	-3.8E-06	-3.9E-06	0
-3.9E-06	-3.9E-06	-4.E-06	-4.E-06	-3.9E-06	-3.9E-06	-3.9E-06	-3.9E-06	-3.9E-06	-3.9E-06	-3.9E-06	-3.9E-06	-3.9E-06	-3.9E-06	-3.9E-06	-3.9E-06	-3.9E-06	-3.9E-06	-3.9E-06	-3.9E-06
-3.9E-06	-3.9E-06	-4.E-06	-4.E-06	-3.9E-06	-3.9E-06	-3.9E-06	-3.9E-06	-3.9E-06	-3.9E-06	-3.9E-06	-3.9E-06	-3.9E-06	-3.9E-06	-3.9E-06	-3.9E-06	-3.9E-06	-3.9E-06	-3.9E-06	-3.9E-06

Table 7.2 – Calibration coefficient matrix *Bin*

MATRIX B																			
1.7E-10	0	0	0	0	0	0	0	0	0	0	0	0	0	0	0	0	0	0	0
1.7E-10	-9.2E-09	0	0	0	0	0	0	0	0	0	0	0	0	0	0	0	0	0	0
-9.4E-09	-9.4E-09	-1.2E-08	0	0	0	0	0	0	0	0	0	0	0	0	0	0	0	0	0
-1.3E-08	-1.3E-08	-1.3E-08	-1.5E-08	0	0	0	0	0	0	0	0	0	0	0	0	0	0	0	0
-1.5E-08	-1.5E-08	-1.5E-08	-1.5E-08	-1.7E-08	0	0	0	0	0	0	0	0	0	0	0	0	0	0	0
-1.7E-08	-1.7E-08	-1.7E-08	-1.7E-08	-1.7E-08	-1.8E-08	0	0	0	0	0	0	0	0	0	0	0	0	0	0
-1.9E-08	-1.9E-08	-1.9E-08	-1.9E-08	-1.9E-08	-1.9E-08	-2.0E-08	0	0	0	0	0	0	0	0	0	0	0	0	0
-2.1E-08	-2.1E-08	-2.1E-08	-2.1E-08	-2.1E-08	-2.1E-08	-2.1E-08	-2.2E-08	0	0	0	0	0	0	0	0	0	0	0	0
-2.2E-08	-2.2E-08	-2.2E-08	-2.2E-08	-2.2E-08	-2.2E-08	-2.2E-08	-2.2E-08	-2.3E-08	0	0	0	0	0	0	0	0	0	0	0
-2.3E-08	-2.3E-08	-2.3E-08	-2.3E-08	-2.3E-08	-2.3E-08	-2.3E-08	-2.3E-08	-2.3E-08	-2.4E-08	0	0	0	0	0	0	0	0	0	0
-2.5E-08	-2.5E-08	-2.5E-08	-2.5E-08	-2.5E-08	-2.5E-08	-2.5E-08	-2.5E-08	-2.5E-08	-2.5E-08	-2.6E-08	0	0	0	0	0	0	0	0	0
-2.7E-08	-2.7E-08	-2.7E-08	-2.7E-08	-2.7E-08	-2.7E-08	-2.7E-08	-2.7E-08	-2.7E-08	-2.7E-08	-2.7E-08	-2.8E-08	0	0	0	0	0	0	0	0
-2.8E-08	-2.8E-08	-2.8E-08	-2.8E-08	-2.8E-08	-2.8E-08	-2.8E-08	-2.8E-08	-2.8E-08	-2.8E-08	-2.8E-08	-2.8E-08	-2.9E-08	0	0	0	0	0	0	0
-2.9E-08	-2.9E-08	-2.9E-08	-2.9E-08	-2.9E-08	-2.9E-08	-2.9E-08	-2.9E-08	-2.9E-08	-2.9E-08	-2.9E-08	-2.9E-08	-2.9E-08	-2.9E-08	-3.0E-08	0	0	0	0	0
-3.1E-08	-3.1E-08	-3.1E-08	-3.1E-08	-3.1E-08	-3.1E-08	-3.1E-08	-3.1E-08	-3.1E-08	-3.1E-08	-3.1E-08	-3.1E-08	-3.1E-08	-3.1E-08	-3.1E-08	-3.2E-08	0	0	0	0
-3.3E-08	-3.3E-08	-3.3E-08	-3.3E-08	-3.3E-08	-3.3E-08	-3.3E-08	-3.3E-08	-3.3E-08	-3.3E-08	-3.3E-08	-3.3E-08	-3.3E-08	-3.3E-08	-3.3E-08	-3.3E-08	-3.3E-08	0	0	0
-3.3E-08	-3.3E-08	-3.3E-08	-3.3E-08	-3.3E-08	-3.3E-08	-3.3E-08	-3.3E-08	-3.3E-08	-3.3E-08	-3.3E-08	-3.3E-08	-3.3E-08	-3.3E-08	-3.3E-08	-3.3E-08	-3.3E-08	-3.4E-08	0	0
-3.4E-08	-3.4E-08	-3.4E-08	-3.4E-08	-3.4E-08	-3.4E-08	-3.4E-08	-3.4E-08	-3.4E-08	-3.4E-08	-3.4E-08	-3.4E-08	-3.4E-08	-3.4E-08	-3.4E-08	-3.4E-08	-3.4E-08	-3.4E-08	-3.5E-08	0
-3.5E-08	-3.5E-08	-3.5E-08	-3.5E-08	-3.5E-08	-3.5E-08	-3.5E-08	-3.5E-08	-3.5E-08	-3.5E-08	-3.5E-08	-3.5E-08	-3.5E-08	-3.5E-08	-3.5E-08	-3.5E-08	-3.5E-08	-3.5E-08	-3.5E-08	-3.6E-08
-3.7E-08	-3.7E-08	-3.7E-08	-3.7E-08	-3.7E-08	-3.7E-08	-3.7E-08	-3.7E-08	-3.7E-08	-3.7E-08	-3.7E-08	-3.7E-08	-3.7E-08	-3.7E-08	-3.7E-08	-3.7E-08	-3.7E-08	-3.7E-08	-3.7E-08	-3.7E-08

Table 7.3 – Calibration coefficient matrix *C_{in}*

MATRIX C																			
6.3E-11	0	0	0	0	0	0	0	0	0	0	0	0	0	0	0	0	0	0	0
6.6E-11	7.7E-09	0	0	0	0	0	0	0	0	0	0	0	0	0	0	0	0	0	0
7.6E-09	7.6E-09	-9.7E-09	0	0	0	0	0	0	0	0	0	0	0	0	0	0	0	0	0
9.0E-09	9.0E-09	9.0E-09	9.8E-09	0	0	0	0	0	0	0	0	0	0	0	0	0	0	0	0
9.7E-09	9.7E-09	9.7E-09	9.7E-09	9.9E-09	0	0	0	0	0	0	0	0	0	0	0	0	0	0	0
9.8E-09	9.8E-09	9.8E-09	9.8E-09	9.8E-09	9.6E-09	0	0	0	0	0	0	0	0	0	0	0	0	0	0
8.9E-09	8.9E-09	8.9E-09	8.9E-09	8.9E-09	8.9E-09	8.3E-09	0	0	0	0	0	0	0	0	0	0	0	0	0
6.7E-09	6.7E-09	6.7E-09	6.7E-09	6.7E-09	6.7E-09	6.7E-09	5.7E-09	0	0	0	0	0	0	0	0	0	0	0	0
5.5E-09	5.5E-09	5.5E-09	5.5E-09	5.5E-09	5.5E-09	5.5E-09	5.5E-09	4.4E-09	0	0	0	0	0	0	0	0	0	0	0
4.4E-09	4.4E-09	4.4E-09	4.4E-09	4.4E-09	4.4E-09	4.4E-09	4.4E-09	4.4E-09	4.4E-09	3.3E-09	0	0	0	0	0	0	0	0	0
2.5E-09	2.5E-09	2.5E-09	2.5E-09	2.5E-09	2.5E-09	2.5E-09	2.5E-09	2.5E-09	2.5E-09	2.4E-09	1.4E-09	0	0	0	0	0	0	0	0
-1.6E-10	-1.6E-10	-1.6E-10	-1.6E-10	-1.6E-10	-1.6E-10	-1.6E-10	-1.6E-10	-1.6E-10	-1.6E-10	-1.6E-10	-1.3E-10	0	0	0	0	0	0	0	0
-1.4E-09	-2.8E-08	-2.8E-08	-2.8E-08	-2.8E-08	-2.8E-08	-2.8E-08	-2.8E-08	-2.8E-08	-2.8E-08	-2.8E-08	-2.8E-08	-2.8E-08	-2.8E-08	0	0	0	0	0	0
-2.5E-09	-2.5E-09	-2.5E-09	-2.5E-09	-2.5E-09	-2.5E-09	-2.5E-09	-2.5E-09	-2.5E-09	-2.5E-09	-2.5E-09	-2.5E-09	-2.5E-09	-2.5E-09	-3.5E-09	0	0	0	0	0
-4.2E-09	-4.2E-09	-4.2E-09	-4.2E-09	-4.2E-09	-4.2E-09	-4.2E-09	-4.2E-09	-4.2E-09	-4.2E-09	-4.2E-09	-4.2E-09	-4.2E-09	-4.2E-09	-4.2E-09	-5.1E-09	0	0	0	0
-6.2E-09	-6.2E-09	-6.2E-09	-6.2E-09	-6.2E-09	-6.2E-09	-6.2E-09	-6.2E-09	-6.2E-09	-6.2E-09	-6.2E-09	-6.2E-09	-6.2E-09	-6.2E-09	-6.2E-09	-6.2E-09	-6.2E-09	-7.1E-09	0	0
-7.2E-09	-7.2E-09	-7.2E-09	-7.2E-09	-7.2E-09	-7.2E-09	-7.2E-09	-7.2E-09	-7.2E-09	-7.2E-09	-7.2E-09	-7.2E-09	-7.2E-09	-7.2E-09	-7.2E-09	-7.2E-09	-7.2E-09	-7.2E-09	-8.0E-09	0
-8.0E-09	-8.0E-09	-8.0E-09	-8.0E-09	-8.0E-09	-8.0E-09	-8.0E-09	-8.0E-09	-8.0E-09	-8.0E-09	-8.0E-09	-8.0E-09	-8.0E-09	-8.0E-09	-8.0E-09	-8.0E-09	-8.0E-09	-8.0E-09	-8.7E-09	0
-9.2E-09	-9.2E-09	-9.2E-09	-9.2E-09	-9.2E-09	-9.2E-09	-9.2E-09	-9.2E-09	-9.2E-09	-9.2E-09	-9.2E-09	-9.2E-09	-9.2E-09	-9.2E-09	-9.2E-09	-9.2E-09	-9.2E-09	-9.2E-09	-9.2E-09	-9.8E-09
-1.0E-08	-1.0E-08	-1.0E-08	-1.0E-08	-1.0E-08	-1.0E-08	-1.0E-08	-1.0E-08	-1.0E-08	-1.0E-08	-1.0E-08	-1.0E-08	-1.0E-08	-1.0E-08	-1.0E-08	-1.0E-08	-1.0E-08	-1.0E-08	-1.0E-08	-1.0E-08

7.2 Experimental in-depth strain relaxation distribution

Table 7.4 shows the strain relaxation-depth values obtained during the experimental procedure described in section 5.2.2, which are used for the validation of minimum and maximum stresses obtained using the MATLAB scripts developed. More precisely, Table 7.4 shows the surface strain relaxation values, corresponding to an applied uniaxial tensile stress of 74 MPa on the selected CFRP specimen (section 5.1), measured in three different directions around the hole, for each depth increment drilled. The three element strain gauge rosettes used during the experimental procedure have strain gauges oriented according to Fig. 5.5.

Table 7.4 Strain-depth relaxation values obtained during the experimental calibration [45]

	Depth (mm)	Strain gauge 1	Strain gauge 2	Strain gauge 3
1	0.05	8	11	0
2	0.10	-77	-12	-4
3	0.15	-83	-10	-12
4	0.20	-87	-9	-20
5	0.25	-126	-6	-26
6	0.30	-167	-3	-30
7	0.36	-171	-1	-36
8	0.41	-174	1	-51
9	0.46	-188	5	-55
10	0.51	-202	10	-55
11	0.56	-205	11	-53
12	0.61	-206	12	-66
13	0.66	-210	16	-61
14	0.70	-213	20	-64
15	0.76	-214	21	-77
16	0.81	-215	21	-77
17	0.86	-215	25	-81
18	0.91	-215	29	-85
19	0.97	-216	29	-87
20	1.02	-216	29	-85

The corresponding strain relaxation-depth curves are shown in Figure 7.5. As expected the greatest strain relaxation values were measured by the strain gauge 1 (see also Figure 5.5), which was oriented with the direction of the applied force of calibration and with the direction of the longitudinal fibres (0°). Minimum values were obtained by the strain gauge 3 that measured the relaxation induced by

the Poisson's effect only. Intermediate values were determined by the strain gauge 2, which was oriented at 45° with the fibres.

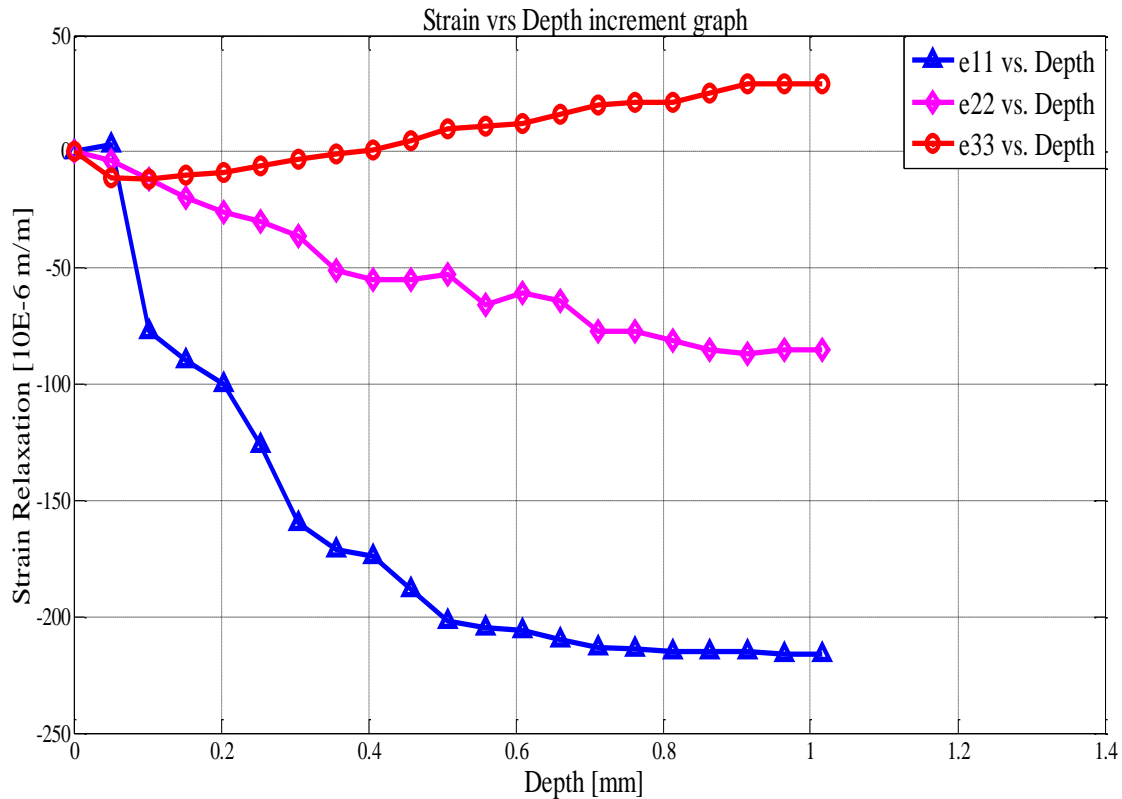


Figure 7.5 Strain relaxation-depth curves generated using the MATLAB code.

The behaviour of the strain-relaxation-depth curves presented in Figure 7.5 are typical curves obtained during the hole-drilling tests in all cases. Since the strains in consideration are the released strains after each depth increment, all curves tend to a constant final value when the released strain correspond to an existing stress far from the surface. It means that, for deeper layers, and independently of the magnitude of stresses existing in those layers, the hole-drilling method becomes unable to measure the correspondent strain release [16]. This loose of sensibility to measure released strains at surface due to existing stresses in depth is an inherent limitation of the hole-drilling method itself. This limits the hole-drilling method for measuring residual stresses for depths greater than the hole radius (in this case equal to ~0.9 mm).

7.3 Calculated stress distribution and validation of the MATLAB scripts developed

The strain relaxation-depth values shown in Table 7.4 and Figure 7.5 were used as input for the calculation procedure implemented by the MATLAB scripts developed in this work. Based on the calibration coefficients previously determined by the finite element method, and shown in Tables 7.1, 7.2 and 7.3, the stresses related with those strain relaxation values can be calculated using the MATLAB developed codes. Figure 7.6 shows the results obtained from the calculation. For comparison purposes only the principal stress values calculated by the developed code are shown.

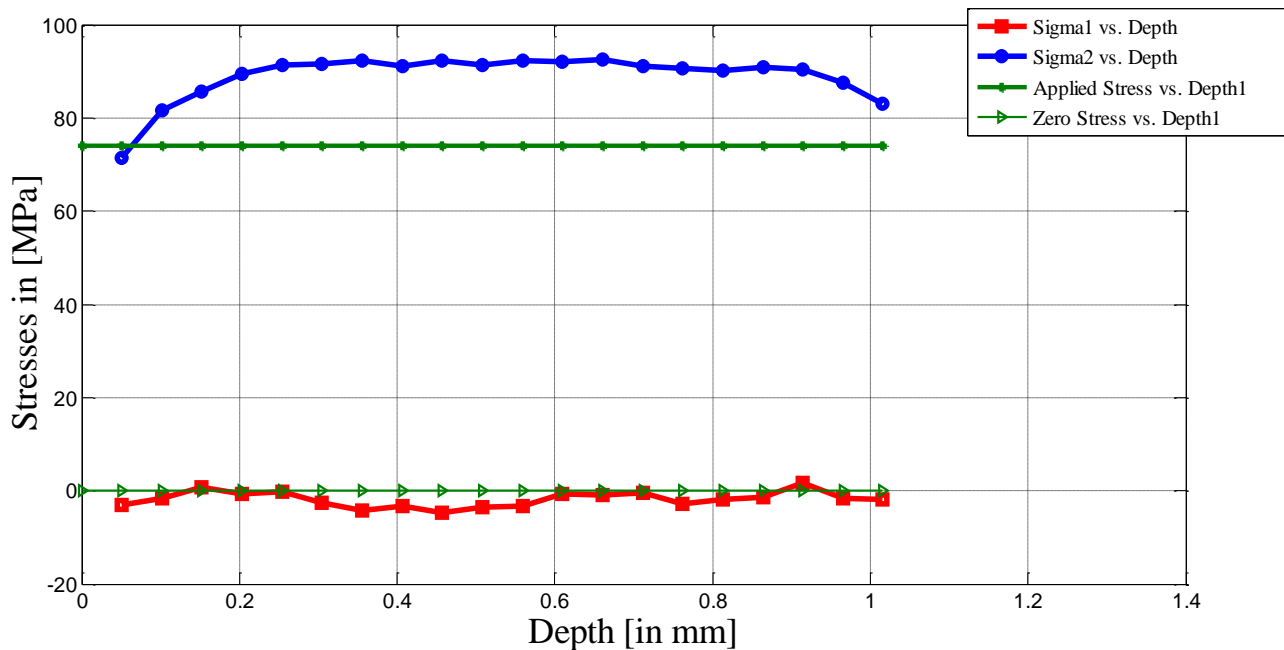


Figure 7.6 Maximum principal stress and minimum principal stress calculated by the MATLAB scripts developed.

The MATLAB scripts developed to implement the calculation procedure for the determination of residual stresses can then be validated. During the experimental procedure [45] a tensile stress of 74 MPa was applied to the specimen during the application of the hole drilling technique. It was expected from the graphs that the results obtained for the principal stress should have an average value close to 74 MPa and the minimum principal stress approaching zero. According to the results presented in Fig. 6.2, the maximum principal stress is greater than the experimentally applied stress over the depth range, while the minimum principal stress is in good agreement with the expected value.

It should be also observed that the maximum principal stress increases during the first depth increments and stabilize after 0.2 mm depth. This stabilized value should correspond to the applied calibration stress of 74 MPa. The initial increase of the maximum principal stresses in the graph suggests there was an error introduced on the results at the beginning of the hole-drilling, i.e., in the first depth increments. This might happen due to the following main factors:

1. The effect of the drill bit geometry used during hole-drilling;
2. The effect of the positioning or centering of the drill bit. Any eccentricity in respect of the centre of the strain gauge rosette induces errors;
3. The surface preparation could contribute directly or indirectly to the results;
4. The effect of the numerical uncertainties on the calibration coefficient matrix determination;
5. The thermo-mechanical effects of the cutting procedure can induce parasitic stresses, especially in the case of fibre reinforce polymers;
6. The limitation of the theoretical approach used for residual stress calculation that was followed.

Of course, assuming that the measurement system gives accurate strain values, the geometric effects due to inaccuracies on the hole diameter and hole depth measurements can be disregarded and finally if the elastic constants of the material were well determined. All these factors are necessary to be considered and accounted for during the laboratory experiments. The difference and variation in the maximum residual stress obtained by the MATLAB developed code should certainly be due to these factors.

For better understand the observed differences between the calculated stresses and the experimental expected stress value, the observed error as a function of the hole depth was determined. This error is the relative difference between the maximum principal stress, calculated by the MATLAB scripts developed, and the expected stress applied during the uniaxial tensile tests (74 MPa). Figure 7.7 presents the results of the error in the determination of the maximum principal stress, since the observed one in the minimum principal stress can be neglected.

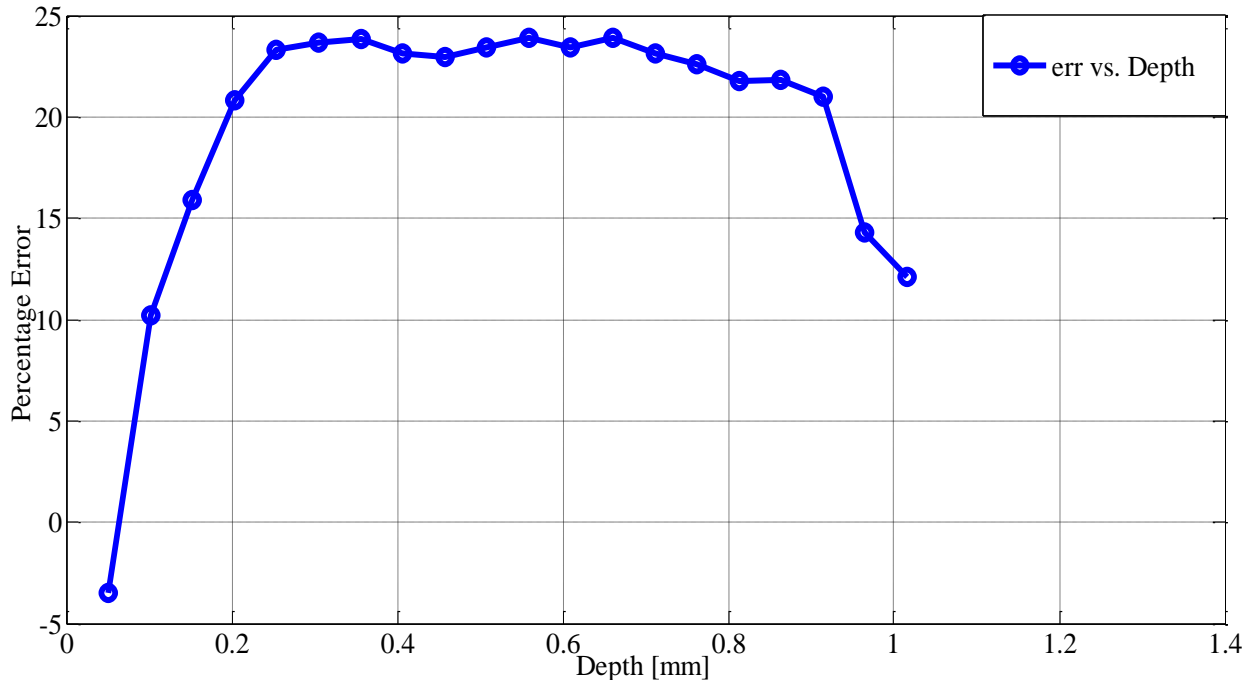


Figure 7.7 Observed error [%] between the maximum principal stress calculated by the MATLAB scripts developed and the expected stress value

As observed, the error increases in the first depth increments and stabilizes in a value around 23%, after a hole depth equal to about 0.2 mm. This average error is too high and the reasons for its appearance should certainly be associated to the factors referred above. A discussion of these factors and their consequences will be performed in the following. However, according to reference [45], were the experimental results used in this work are reported, the factors 2 and 3 pointed out above can be disregarded. Therefore, the discussion will be essentially focused in the reasons 1, 4, 5 and 6, which should be directly related with the observed differences between the calculated stress and the experimental value, used as reference.

7.3.1 Effect of the drill bit geometry

The end mills for the incremental hole-drilling technique usually present a small chamfer, which can affect the hole shape, especially in the first depth increments. This means that the real shape of the drilled hole is not perfectly cylindrical, as it can be seen in the micrograph of Figure 7.8, taking from reference [45], where the experimental results used in this work were reported. In Figure 7.8, it is

clear that a small portion of the material remains, since it is not cut during hole-drilling due to the end mill chamfer.

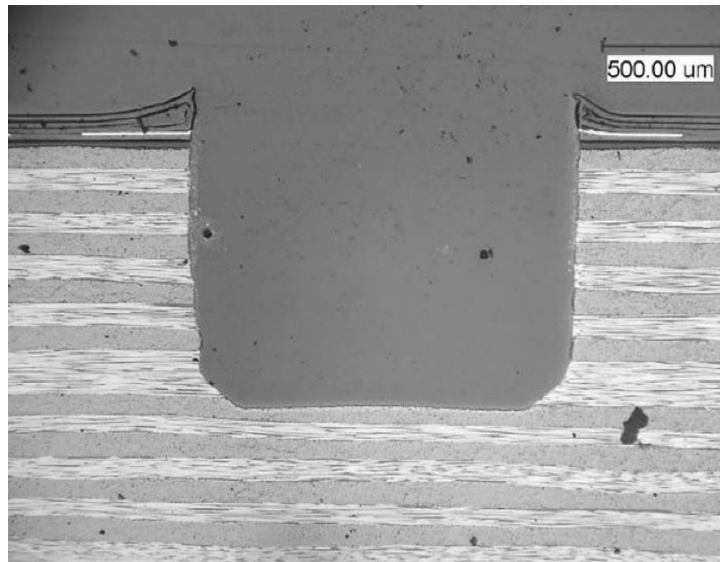


Figure 7.8 Micrograph of drilled hole showing the remaining portion which was not removed [45]

The effect of the chamfer is more pronounced during the first depth increments than in the deeper ones, since the effect of the chamfer decreases with the increase of the hole size. Its effect on the results of the stress calculation procedure is related with the fact that, during the numerical simulation by FEM to obtain the calibration constants A_{in} , B_{in} and C_{in} , a pure cylindrical shape for the hole is assumed. Therefore, for the first depth increments, the amount of material cut is smaller than if a pure cylindrical shape is assumed. This effect decreases with the increase of the hole depth. Hence, this effect can justify the shape of the maximum principal stresses curve shown in Figure 7.6 for the first depth increments. However, the magnitude of the calculated stress and the high observed error should be associated to other effects.

7.3.2 Effect of the numerical uncertainties on the calibration coefficient matrix determination

It is clear from Figure 7.6 that, for deeper layers, the maximum principal stress remains at values ranging from 88 MPa to 93 MPa and the minimum stresses settle approximately close to the expected result. The reason for the average maximum principal stresses being higher than the applied stress, leading to an error of 23% can be attributed to the numerical uncertainties on the determination of the

calibration coefficients matrices A_{in} , B_{in} and C_{in} , respectively, from Tables 7.1, 7.2 and 7.3. Numerical inaccuracies in their determination affect the calculated results of the stresses, since the stresses are directly dependent on these coefficients.

7.3.3 Thermo-mechanical effects of the cutting procedure

Considering the results presented in reference [4], the thermo-mechanical effects due to the cutting procedure should certainly have influence on the experimentally determined strain relaxation-depth curves, hence affecting the stress calculation using the MATLAB code developed in this work. This issue should be better investigated in the future. Although the average maximum stress obtained is higher than the applied stress, the trend presents very promising indicator about the development of the incremental hole-drilling technique for measuring residual stresses in composite laminates. Probably, if the real shape of the hole was considered during the finite element analysis, thus correcting the values of the calibration coefficients, the final stress value could be perfectly constant. This explanation of the findings should, however, be ascertained in future works.

7.3.4 Limitation of the theoretical approach used for residual stress calculation

Finally, a reference to the theoretical approach followed to develop the MATLAB code [3, 5] should be done. The theoretical approach followed in this work is based on a simple approach, assuming that the relieved strain response has a similar trigonometric form to that observed in an isotropic material, as it can be seen in equation (1). Equation (1) is assumed still to apply, providing that gauges 1 and 3 are aligned along the elastic symmetry directions of the orthotropic material, as it happened in the composite material previously used. In this case, constant C is an independent calibration constant, not related to A or B, as it happens for isotropic materials. The use of equation (1) was suggested for hole-drilling applications by several authors [35, 37]. However, Schajer and Yang [34] have shown that the use of equation (1) can imply final errors in residual stress calculation because the displacement field around a hole, in a stressed orthotropic plate, does not have a simple trigonometric form. Figure 7.9 shows differences that can be expected in the normalized relieved strain around the hole in an orthotropic plate, comparatively to what is expected in an isotropic material. The differences increase with the increase of the orthotropy ratio is E_{11}/E_{22} . In the case of the composite laminate used in this study, this ratio attains 47.

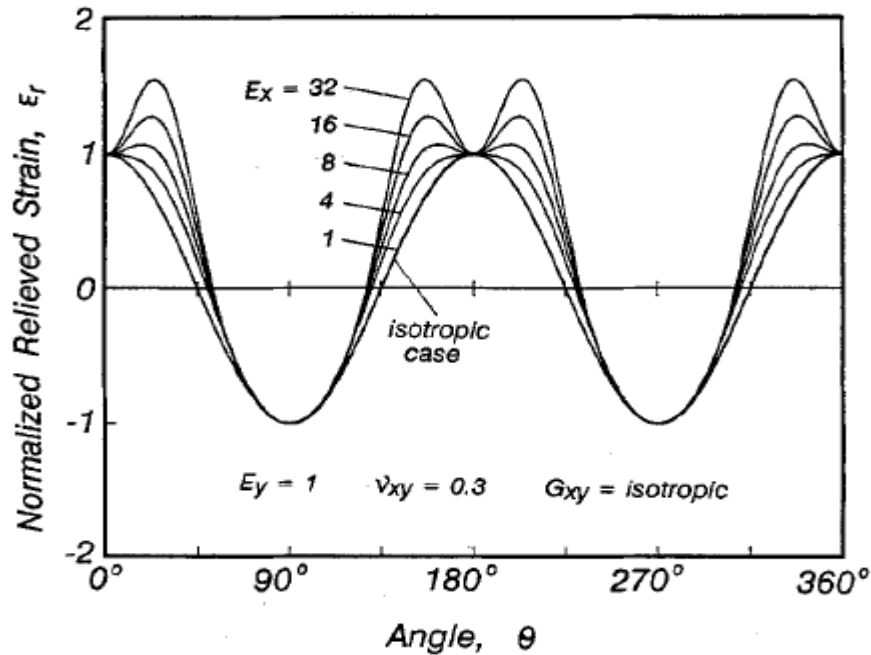


Figure 7.9 Angular variation of relieved strain in materials of varying degrees of axial orthotropy [34].

Disregarding the first depth increments, where the calculated stress values are affected by the end mill chamfer effect, an error of around 23% was observed. The reason for this level of error should be studied in the future, regarding the effect of the factors discussed above. However, higher errors have already been reported by other authors. Schajer and Yang [34], for example, during their calibration tests, recorded stress-measurement errors in the 10-20-percent range. According to these authors, this error range was expected to be typical of hole-drilling measurements in orthotropic laminates. Accuracy of the final results is strongly dependent on the measurement procedure and on the algorithms adopted to calculate the stresses.

8. CONCLUSIONS

In this work, scripts using MATLAB were developed for determining residual stresses in orthotropic composite laminates. The theoretical approach followed was proposed by Sicot et al. [3, 5]. This approach enables to determine the in-depth non uniform residual stress based on the relieved strains measured during the application of the incremental hole-drilling technique to orthotropic composite

laminates. Considering the case of carbon-fibre reinforced polymer (CFRP) specimens, with the stacking sequence $[0_0, 90_0]_5$ the necessary calibration coefficient matrices, related with the residual calculation procedure used, were determined by the finite element method.

For validation purposes, the results obtained in an experimental study, previously performed to the present work, were used. The strain relaxation-depth curves reported in that study, corresponding to above mentioned specimens, when subjected to a well-known uniform uniaxial stress, were used as input data for the MATLAB scripts developed in this work.

Differences between the applied experimental stress (uniform stress) and the calculated one, by using the MATLAB code developed, were observed. The level of the observed error (~23%) was high, but similar level of errors were also referred by other authors, reporting experimental calibration procedures using the hole-drilling technique in composite laminates. Beyond the problems related with the theoretical approach followed, the source of errors must be well study in the future. The effect of the chamfer of the drill bits, the thermomechanical effects of the cutting process, the laminar structure of most orthotropic materials, the uncertainty of local elastic properties and the angular misalignment of the strain-gauge rosette relative to the material principal elastic directions, are common sources of errors. However, considering the results obtained in this work, the incremental hole-drilling can be considered a promising technique for residual stress measurement in composite laminates.

9. REFERENCES

- [1] Tsouvalis, N., Margelis, G., Dellis, D., “Residual stresses in composite materials: a review”, NTUA Report No MAR-R4-3-NTUA-24(2) for MARSTRUCT, January 2009.
- [2] Cherouat A., Gong X.L., Sicot O. and Lu J., “Influence of the Residual Stresses on the mechanical behavior of advanced composite parts”, *Journal of Neutron Research*, 9(2), 319-330 (2001).
- [3] Sicot, O., Gong, X., Cherouat, A., Lu, J., “Determination of residual stress in composite laminates using the hole-drilling method”, *J. Comp. Mat.*, 37, 831–844 (2003).
- [4] Nobre, J.P., Stiffel, J.H, Nau, A., Outeiro, J., Batista, A.C., Induced drilling strains in glass fibre reinforced epoxy composites. *CIRP Annals Manufacturing Technology*, 62(1), 87-90 (2013).
- [5] Sicot, O., Gong, X.L., Cherouat, A., Lu J., “Determination of Residual Stress in Composite Laminates using the Incremental Hole-drilling Method”, *J. Comp. Mat.*, 37, 831–844 (2003).
- [6] Parlevliet, P.P., Bersee, H.E.N., Beukers, A, “Residual stresses in thermoplastic composites- A study of the literature – Part 1: Formation of residual stresses”, *Composite: Part A*, 37, 1847 – 1857 (2006).
- [7] Kim, K., Hahn, H. and Croman, R., “The effect of cooling rate on residual stresses in a thermoplastic composite”, *J. Compositre Technol. Res.*, 11(2), 47-52 (1998).
- [8] Daniel, I.M., Liber, Theodore, “Lamination residual stresses in fiber composites”, *NASA- CR-134826*, 1975.
- [9] While, S.R. and Hahn, H.T. “Process modeling of composites materials: residual stress development during cure. Part I - Model formulation”, *J. Comp. Mat.*, 26, 402-2422 (1992).
- [10] Kharkhadi S, Abrol N, Somani P., Sharma A., Singh T., “Review on Fiber Reinforced Polymer” *International Journal of Combined Research & Development (IJCRD)* eISSN: 2321-225X ; pISSN:2321-2241 Volume: 4; Issue: 6; June -2015
- [11] Hinton M.J., Soden P.D., Kaddour A.S., “Failure Criteria in Fibre-Reinforced-Polymer Composites: The World-Wide Failure Exercise”, Elsevier, 2004.
- [12] Masuelli, M. A, Introduction of Fibre-Reinforced Polymers, Polymers and Composites: Concepts, Properties and Processes. ISBN 978-953-51-0938-9, Published: January 23, 2013 under CC BY 3.0 license. © The Author(s)
- [13] Reid R. G., Paskaramoorthy R. An extension to classical lamination theory for use with functionally graded plates, *Composite Structures*, 93(2): 639-648, 2011

- [14] Williams G., Trask R., Bond I., “A self-healing carbon fibre reinforced polymer for aerospace applications”, Part A 38 (2007) 1525–1532. University of Bristol, Queen’s Building, University Walk, Bristol BS8 1TR, UK, Received 17 May 2006; received in revised form 16 November 2006; accepted 7 January 2007.
- [15] Chen B. T. Yeh H. C. & Hobbs C. H. “Size Classification of Carbon Fiber Aerosols, Aerosol Science and Technology”, (1993), 19:2, 109-120, DOI: 10.1080/02786829308959625
- [16] Nobre, J.P., Batista, A.C., Nau, A, Paeppegem, W.V, and Scholtes, B., “Using the incremental hole-drilling technique for measuring residual stresses in fibre-reinforced polymer composites”, Proc. 5th European Conference on Composite Materials, Venice, July 2011, Italy, pp 1 – 8, 2011.
- [17] Gary S. Schajer, Michael B. Prime, “Use of inverse solutions for residual stress measurement”, January 2005, Los Alamos National Laboratory, Engineering Sciences and Applications Division, LA-UR-04-5890, *Journal of Engineering Materials and Technology*, 128(3), 375-382 (2006).
- [18] Patricia P. Parlevliet, Harald E.N. Bersee, Adriaan Beukers, “Residual stresses in thermoplastic composites – A study of the literature – Part II: Experimental techniques”, *Composites: Part A*, 38, 651-665 (2006).
- [19] Olabi A.G., Hashmi M.S.J., “Stress relief procedures for low carbon steel (1020) welded components”, *J. Eng. Mater. Tech.*, 56, 552-562 (1996).
- [20] Kandil, F., Lord, J., Fry, A., Grant, P., “A review of residual stress measurement methods, a guide to technique selection”, NPL Report MATC(A)04, UK, 2001.
- [21] Stamatopoulos K., “Measurement of residual stresses in composite materials with the incremental hole drilling method”, Athens, June 2011.
- [22] Milbradt K.P., “Ring-method determination of residual stresses”, Proc SESA, 9(1), 63–74 (1951).
- [23] Kiel S., “Experimental determination of residual stresses with the ring-core method and an online measuring system”, *Exp. Tech.*, 16(5): 17–24 (1992).
- [24] Ajovalasit, A., Petrucci, G., Zucarello, B. “Determination of Nonuniform Residual Stresses Using the Ring-Core Method”, *J. Eng. Mater. Tech.*, 118(2), 224-228 (1996).
- [25] Prime M.B., “Residual stress measurement by successive extension of a slot: the crack compliance method”, *Appl. Mech. Rev.*, 52(2), 75–96 (1999).

- [26] Germaud M., Cheng W., Finnie I., Prime M.B., “The compliance method for measurement of near surface residual stresses analytical background”, *J. Eng. Mater. Tech.*, 119(4), 550–555 (1994).
- [27] Cheng W., Finnie I., “Residual stress measurement and the slitting method”. New York: Springer 2007, ISBN 978-144194241.
- [28] Cowley K.D. and Beaumont P.W.R., “The measurement and prediction of residual stresses in carbon-fibre/polymer composites”, *Composites Science and Technology*, 57(11), 1445–55 (1997).
- [29] Leggatt R.H, Smith D.J., Smith S.D., Faure F., “Development and experimental validation of the deep hole method for residual stress measurement”, *J. Strain Anal.*, 31(3), 177–186 (1996).
- [30] Bateman M.G., Miller O.H., Palmer T.J., Breen C.E.P., Kingston E.J., Smith D.J., Pavier M.J. “Measurement of residual stress in thick section composite laminates using the deep-hole method”, *Int. J. Mech. Sci.*, 47, 1718–1739 (2005).
- [31] Sachs G. “Der nachweis innerer spannungen in stangen und rohren”, *Zeitschrift fur Metallkunde*, 19, 352–357 (1972).
- [32] Oettel R., “The determination of uncertainties in residual stress measurement (using the hole drilling technique)”, Issue 1, September 2000, Manual of Codes of Practice for the determination of uncertainties in mechanical tests on metallic materials, Code of Practice No. 15, Standards Measurement & Testing Project No. SMT4-CT97-2165.
- [33] ASTM E 837-13, “Standard Test Method For Determining Residual Stresses By Hole Drilling Gage Method”, ASTM, West Conshohocken, United State, 2013.
- [34] Schajer G.S and Yang L., “Residual-Stresses Measurement in Orthotropic Materials Using the Hole-drilling Method”, *Exp. Mech.*, 34(4), 324-333 (1994).
- [35] Bert, C.W. and Thompson, G.L. "A Method for Measuring Planar Residual Stresses in Rectangularly Orthotropic Materials", *J. Comp. Mat.*, 2(2), 244-253 (1968).
- [36] Lake, B.R., Appl, F.J. and Bert, C.W., “An investigation of the hole-drilling technique for measuring planar residual stress in rectangular orthotropic materials”, *Exp Mech.*, 10 (10), 233-239 (1970).
- [37] Prasad, C.B., Prabhakaran, R. and Thompkins, S., “Determination of Calibration Constants for the Hole-Drilling Residual Stress Measurement Technique Applied to Orthotropic Composites”, *Composite Structures*, Part 1: Theoretical Considerations, 8(2), 105-118 (1987); Part H: Experimental Evaluations, 8 (3), 165-172 (1987).
- [38] Soete, W., “Measurement and Relaxation of Residual Stress”, *Sheet Met. Ind.*, 26(266), 1269–1281 (1949).

- [39] Lake, B.R., F.J. and Bert, C.W., “An Investigation of the Hole-Drilling Technique for Measuring Planar Residual Stress in Rectangular Orthotropic Materials”, *Exp. Mech.*, 10, 233–239 (1970).
- [40] George Margelis, Konstantinos Stamatopoulos, Nicholas Tsouvalis, “Measurement of Residual Stresses in Typical Marine Composite Materials Using the Incremental Hole Drilling Method” NTUA Report No MAR-R4-3-NTUA-28(1) for MARSTRUCT, January 2010.
- [41] Vishay precision group, “Micro measurements,” Vishay precision group, 01 November 2010. [Online]. Available: <http://www.vishaypg.com/doc?11053>. [Accessed 25 November 2015]
- [42] N.N: www.hexcel.com, product data - hexPly M18, demand in March 2010.
- [43] Tavernier, B., Verbeke, T., Health Monitoring of Carbon-Epoxy Laminates Used in Space Applications by Means of Embedded Optical Fibers, Master Thesis, Ghent University, Belgium, 2006.
- [44] Jose, S., Ramesh Kumar, R., Jana, M.K., Venkateswara Rao, G., “Intralaminar Fracture Toughness of a Cross-Ply Laminate and its constituent Sub-Laminates”, *Composite Science and Technology*, 61, 1115-1122 (2001).
- [45] Nobre, J.P., internal report, University of Coimbra, 2011.
- [46] Handbook of Measurement of Residual Stresses. Edited by J. Lu, Society for Experimental Mechanics (SEM), Bethel, 1996.

10. APPENDIX

A1. MATLAB code for the calculation of relieve strains and the corresponding stresses

```
format short e
Amn=[-4.50E-08,-1.10E-06,-1.60E-06,-2.10E-06,-2.40E-06,-2.70E-08,-3.00E06,...
      -3.20E-06,-3.40E-06,-3.50E-06,-3.60E-06,-3.70E-06,-3.70E-06,-3.80E-06,...
      -3.80E-06,-3.80E-06,-3.80E-06,-3.90E-06,-3.90E-06,-3.90E-06];

Bmn=[1.67E-10,-9.20E-09,-1.20E-08,-1.50E-08,-1.70E-08,-1.80E-08,-2.00E-08,...
      -2.20E-08,-2.30E-08,-2.40E-08,-2.60E-08,-2.80E-08,-2.90E-08,-3.00E-08,...
      -3.20E-08,-3.30E-08,-3.40E-08,-3.50E-08,-3.60E-08,-3.70E-08];

Cmn=[6.33E-11,7.71E-09,-9.73E-09,9.79E-09,9.88E-09,9.63E-09,8.27E-09,...
      5.69E-09,4.44E-09,3.33E-09,1.38E-09,-1.30E-10,-2.80E-08,-3.50E-09,...
      -5.10E-09,-7.10E-09,-8.00E-09,-8.70E-09,-9.80E-09,-1.00E-08];

Depth = [0.0508,0.1016,0.1524,0.2032,0.2540,0.3048,0.3556,0.4064,0.4572,...
          0.5080,0.5588,0.6096,0.6604,0.7112,0.7620,0.8128,0.8636,0.9144,...
          0.9652,1.0160]';

Emn=[8,0,-11;-77,-4,-12;-83,-12,-10;-87,-20,-9;-126,-26,-6;-167,-30,-3;...
     -171,-36,-1;-174,-51,1;-188,-55,5;-202,-55,10;-205,-53,11;-206,-66,12;...
     -210,-61,16;-213,-64,20;-214,-77,21;-215,-77,21;-215,-81,25;-215,-85,29;...
     -216,-87,29;-216,-85,29];

Emn1 = Emn(:,1)';
Emn2 = Emn(:,2)';
Emn3 = Emn(:,3)';

for n = 1:20
    e1 = Emn1(:,n)-sum(Emn1(:,1:1:n-1));
    e2 = Emn2(:,n)-sum(Emn2(:,1:1:n-1));
    e3 = Emn3(:,n)-sum(Emn3(:,1:1:n-1));

    An = Amn(1,n);
    Bn = Bmn(1,n);
    Cn = Cmn(1,n);

    theta=0.5*atan((Cn*(e3-e1)-Bn*(2*e2-e1-e3))/(Cn*(2*e2-e1-e3)+Bn*(e3-e1)));
    Sigma1 = (e1*(An-Bn*sin(2*theta)+Cn*cos(2*theta))-e2*(An-Bn*cos(2*theta)-
        Cn*sin(2*theta)))/((2*An*Bn)*(sin(2*theta)+cos(2*theta))+(2*An*Cn)*(sin(2*theta)+cos(2*theta)));
    Sigma2=(e1*(An+Bn*sin(2*theta)+Cn*cos(2*theta))+e2*(An+Bn*cos(2*theta)+Cn*sin(2*theta)))/((2*An*Bn)*(sin(2*theta)+cos(2*theta))+(2*An*Cn)*(sin(2*theta)+cos(2*theta)));

    disp([Sigma1,Sigma2])
end
```

A2. MATLAB code for plotting of Stresses with Depth

```
% Plot of the first set of strain values
format short e
Sigma1=[-0.0309e+10,-0.1737e+09, 0.0655e+09, -0.0752e+09,-0.0111e+09,...
        -0.2552e+09, -0.4121e+09, -0.0339e+10,-0.0478e+10,-0.0347e+10,...
        -0.0333e+10,-0.0079e+10,-0.0089e+10,-0.0038e+10,-0.0275e+10,...
        -0.0187e+10,-0.0140e+10,0.0165e+10,-0.0170e+10,-0.0182e+10]'.*10^-8;

Sigma2=[0.7143e+10,0.8155e+10,0.8577e+10,8.9421e+09,9.1271e+09,...
        0.9152e+10,9.2379e+09, 0.9114e+10, 0.9241e+10,0.9133e+10,...
        0.9241e+10,0.9208e+10,0.9243e+10,0.9111e+10,0.9074e+10,...
        0.9011e+10,0.9090e+10,0.9029e+10, 0.8758e+10,0.8295e+10]'.*10^-8;

Sig1=[74,74,74,74,74,74,74,74,74,74,74,74,74,74,74,74,74,74,74,74]';

Sig2=[0,0,0,0,0,0,0,0,0,0,0,0,0,0,0,0,0,0,0,0]';

Depth = [0.0508,0.1016,0.1524,0.2032,0.2540,0.3048,0.3556,0.4064,0.4572,...
        0.5080,0.5588,0.6096,0.6604,0.7112,0.7620,0.8128,0.8636,0.9144,...
        0.9652,1.0160]';

Depth1 = [0,0.0508,0.1016,0.1524,0.2032,0.2540,0.3048,0.3556,0.4064,0.4572,...
        0.5080,0.5588,0.6096,0.6604,0.7112,0.7620,0.8128,0.8636,0.9144,...
        0.9652,1.0160]';

plot(Depth,Sigma1,'x--',Depth,Sigma2,'og--',Depth1,Sig1,Depth1,Sig2),grid
xlabel('Depth [in mm]')
ylabel(' Stresses in [MPa]')
```

A3. MATLAB code for plotting of the strains with depth

```
%The plot of first set of strain values

A=[8,0,-11;-77,-4,-12;-83,-12,-10;-87,-20,-9;-126,-26,-6;-167,-30,-3;...
-171,-36,-1;-174,-51,1;-188,-55,5;-202,-55,10;-205,-53,11;-206,-66,12;...
-210,-61,16;-213,-64,20;-214,-77,21;-215,-77,21;-215,-81,25;-215,-85,29;...
-216,-87,29;-216,-85,29]';

e11=[0,3,-77,-90,-100,-126,-160,-171,-174,-188,-202,-205,-206,-210,-213,-214,...
-215,-215,-215,-216,-216]';
e22=[0,-4,-12,-20,-26,-30,-36,-51,-55,-55,-53,-66,-61,-64,-77,-77,-81,-85,-87,-
85,-85]';
e33=[0,-11,-12,-10,-9,-6,-3,-1,1,5,10,11,12,16,20,21,21,25,29,29,29]';

Depth = [0,0.0508,0.1016,0.1524,0.2032,0.2540,0.3048,0.3556,0.4064,0.4572,...
        0.5080,0.5588,0.6096,0.6604,0.7112,0.7620,0.8128,0.8636,0.9144,...
        0.9652,1.0160]';

plot(Depth,e11,'x--',Depth,e22,'g--',Depth,e33,'or--'),grid
xlabel('Depth [mm] ')
ylabel('Strain Relaxation [micro m/m]')
title('Strain vrs Depth increment graph')
```

A4. MATLAB code for plotting of Percentage Errors with depth

```
% Percentage error
format short e
err=[-3.4730e+00,1.0203e+01,1.5905e+01,2.0839e+01,2.3339e+01,2.3676e+01,...
     2.3836e+01,2.3162e+01,2.2932e+01,2.3419e+01,2.3878e+01,2.3432e+01,...
     2.3905e+01,2.3122e+01,2.2622e+01,2.1770e+01,2.1838e+01,2.1014e+01,...
     1.4297e+01,1.2095e+01]';

Depth = [0.0508,0.1016,0.1524,0.2032,0.2540,0.3048,0.3556,0.4064,0.4572,...
         0.5080,0.5588,0.6096,0.6604,0.7112,0.7620,0.8128,0.8636,0.9144,...
         0.9652,1.0160]';

plot(Depth,err,'o--'),grid

xlabel('Depth [mm]')
ylabel('Percentage Error')
```